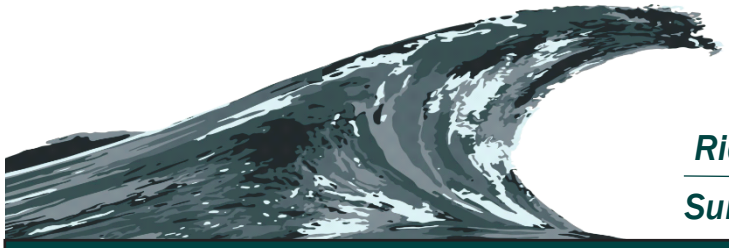

Riding the waves of change

Surfer sur la vague du changement

GAC–MAC–IAH-CNC–CSPG

HALIFAX 2022 May 15-18•15-18 Mai

FIELD TRIP GUIDEBOOK – A5

Volcanism of the Late Silurian Eastport Formation of the Coastal Volcanic Belt, Passamaquoddy Bay, New Brunswick

Leaders: Nancy Van Wagoner, Les Fyffe, David Lentz

GEOLOGICAL ASSOCIATION OF CANADA
ASSOCIATION GÉOLOGIQUE DU CANADA

MINERALOGICAL ASSOCIATION OF CANADA
ASSOCIATION MINÉRALOGIQUE DU CANADA

CNC - SNC
International Association of Hydrogeologists
Association internationale des hydrogéologues

CSPG
Canada's Energy Geoscientists

ATLANTIC GEOSCIENCE SOCIETY

Field Trip Stops

The order of the field trip stops will be dictated by the Bay of Fundy tides. Sites may be added or deleted as time and tides permit and stops are shown by name rather than sequence. Sites were selected based on quality of the exposure, access, and to represent the variety of volcanic facies comprising the sequence. Stops are generally in order from oldest to youngest but there is overlap in the traverses.

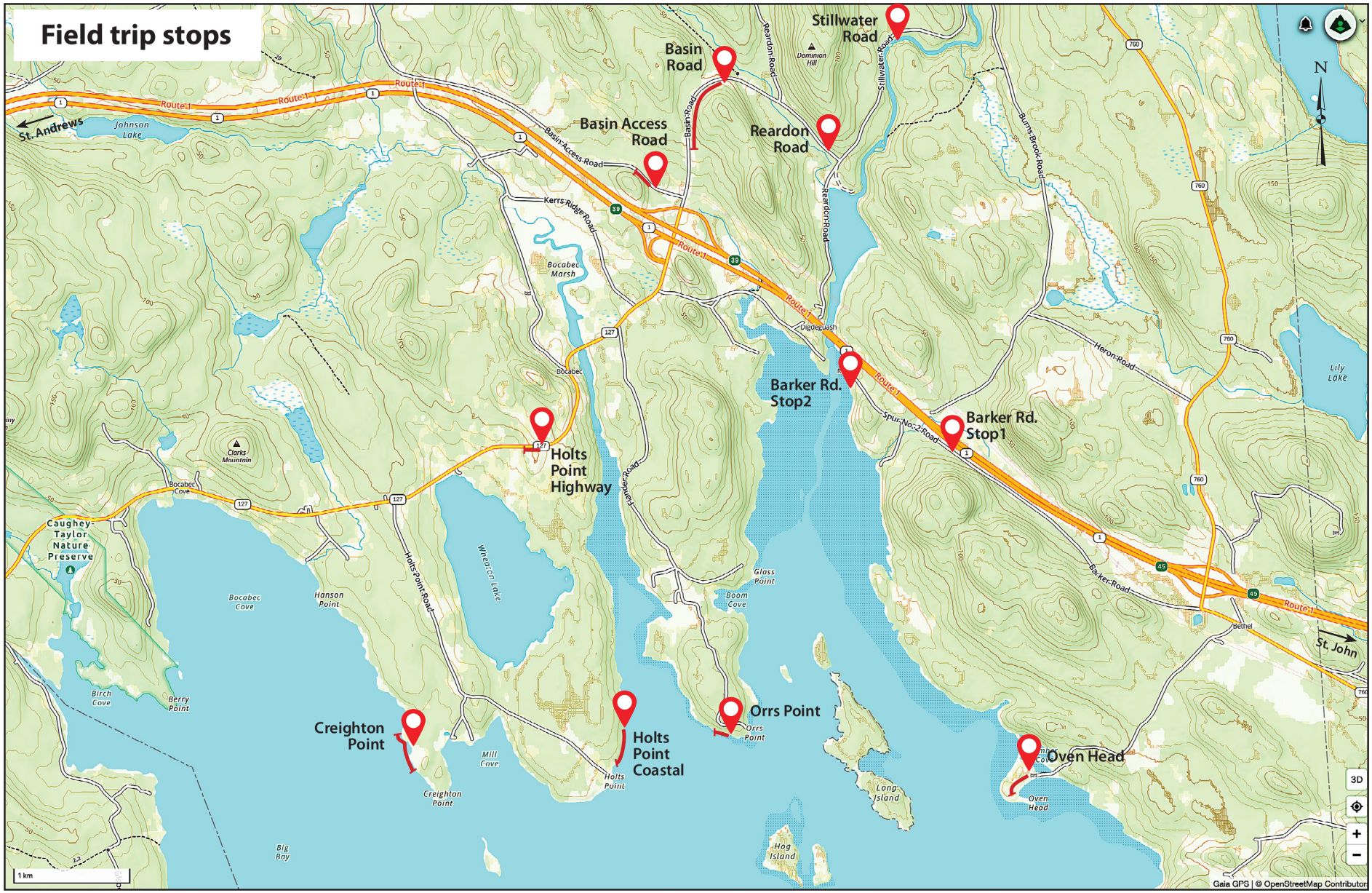

Volcanism of the Late Silurian Eastport Formation of the Coastal Volcanic Belt, Passamaquoddy Bay, New Brunswick

Nancy Van Wagoner[1]*, Les Fyffe[2], David Lentz[3], Kelsie Dadd[4], Wayne McNeil[5], and Diane Baldwin[6]

[1]Thompson Rivers University, Department of Physical Sciences, Kamloops, British Columbia, V2C 0C8
[2]Director, New Brunswick Geological Surveys Branch (retired)
[3]Department of Earth Science, University of New Brunswick, Fredericton, NB, E3B 5A3
[4] School of Geosciences, University of Sydney, Sydney, Australia 2006
[5] 25 Alderney, Dartmouth, Nova Scotia, B2Y 0E4
[6]Minex Services, 17 Gitzel St., Yellowknife, Northwest Territories X1A 2C1

*Email: nvanwagoner@tru.ca

AGS Special Publication Number 60
ISBN 978-1-987894-16-5

Contents

The following stops are not included in this field guide but will be added if time and tides permit. Hand outs will be available during the field trip.

- Fiander Road
- Route 127: Traverse through Cycles 2 and 3
- Bocabec Cove South: Cycle 4 Basalt flows
- Sandy Point: Cycle 4: Sediments and basalt flows of waning volcanism

Note: This field guide was prepared for a guided field trip.

A more complete, self-guided field guide is in preparation. If interested please contact Nancy Van Wagoner at nancy@terragraphic.ca

Safety and Comfort

- During this field trip we will be working along cliff sections of the coast of Passamaquoddy Bay of the Bay of Fundy, and inland roads. Participants are required to wear hard hats around road cuts, cliffs, quarries or other sites where there is an overhead hazard. We will have hard hats for you but please feel free to bring your own as it might be more comfortable.
- We will be walking along the coast where the rocks are wet and covered with seaweed making for extremely slippery and unstable conditions. We will also be climbing over the outcrop. Wear good boots. Waterproof boots are recommended. The GAC and MAC also recommend steel-toed safety boots when working around road cuts and cliffs. Hiking poles may be used to improve stability. We will be traversing at a pace that is comfortable for the group.
- Please bring leather gloves or something similar as the rocks are sharp.
- Long pants and long-sleeved shirts are required to help prevent cuts and scrapes. The rocks are sharp and jagged.
- The weather in May is unpredictable. It might be cold and wet or sunny and glorious. Bring enough foul weather gear to keep you warm and dry, and dress in layers.
- Bring your own safety glasses, rock hammer, and other related field gear.
- We have selected roadcut sections where there is little traffic. Even so, always stay well off the road and watch for traffic when observing and taking photos of the outcrops.
- The Bay of Fundy boasts the largest tides in the world. Coastal stops are planned during low tide, but the tide will be either rising or falling. Always stay with the field trip leaders. We don't want anyone to become trapped by the rising tide.
- We will endeavour to make formal restroom stops, but a small supply of personal hygiene items, and hand sanitizer are recommended.
- It is vital that everyone feels comfortable on this field trip. Please be respectful of others and value the diversity of views and perspectives that may be presented during this field trip.
- While we have a planned itinerary, please keep in mind that we may have to make adjustments due to unforeseen circumstances and the Bay of Fundy tides.
- COVID-19: We will follow the regulations in effect at the time of the field trip. Face masks are recommended and may be required.
- Please raise any concerns with the field trip leaders.

Late Silurian to Early Devonian bimodal (basaltic-rhyolitic) volcanism is a common feature of the northern Appalachians, forming three main belts: the Central Volcanic Belt of Maine (formerly the Piscataquis volcanic belt); the Tobique Volcanic Belt in central New Brunswick and Quebec; and the Silurian Coastal Volcanic Belt. The Coastal Volcanic Belt extends from the southern coast of Maine to the Passamaquoddy Bay coast of southwestern New Brunswick (Fig. 1). Together, these magmatic belts represent a large igneous province, with evidence for super volcano-scale eruptions (Seaman et al., 1999, 2019).

This field trip is a geotraverse through the exquisite, nearly pristine exposures of the Late Silurian, bimodal volcanic and sedimentary sequence of the Eastport Formation in the Passamaquoddy Bay area of southwestern New Brunswick (NB), which forms the northern extent of the Coastal Volcanic Belt (Fig. 1).[1] Here, the Eastport Formation (Passamaquoddy Bay Volcanic Sequence) has a minimum thickness of about 4 km, covers an area of about 185 km^2, and preserves at least four cycles of basaltic-rhyolitic volcanic rocks, intercalated with sedimentary rocks (Figs. 2, 3, 4). The lowest part of the sequence is not seen as it is intruded in the north by the St. George Batholith. The middle and upper parts of the sequence are unconformably overlain in the south by the alluvial clastic rocks of the Late Devonian Perry Formation, and are truncated on the eastern margin by the St. George fault. The upper part of the sequence is bound to the west by the St. Croix fault and the St. Croix River (Fyffe and Fricker, 1987). Exposures are excellent along coastal cliff faces and road cuts, metamorphic grade is low (mostly subgreenschist facies), deformation is minimal, and primary volcanic and sedimentary textures and structures are well preserved.

In addition to being bimodal, the volcanic rocks are subalkaline, and have within-plate tectonic affinity (Fig. 4). The basaltic rocks were interpreted to be partial melts of a subduction modified mantle further influence by crustal contamination, with the rhyolitic rocks being crustal melts, modified by crystal fractionation. Evidence for interaction between mafic and felsic melts and their field associations, suggests that the

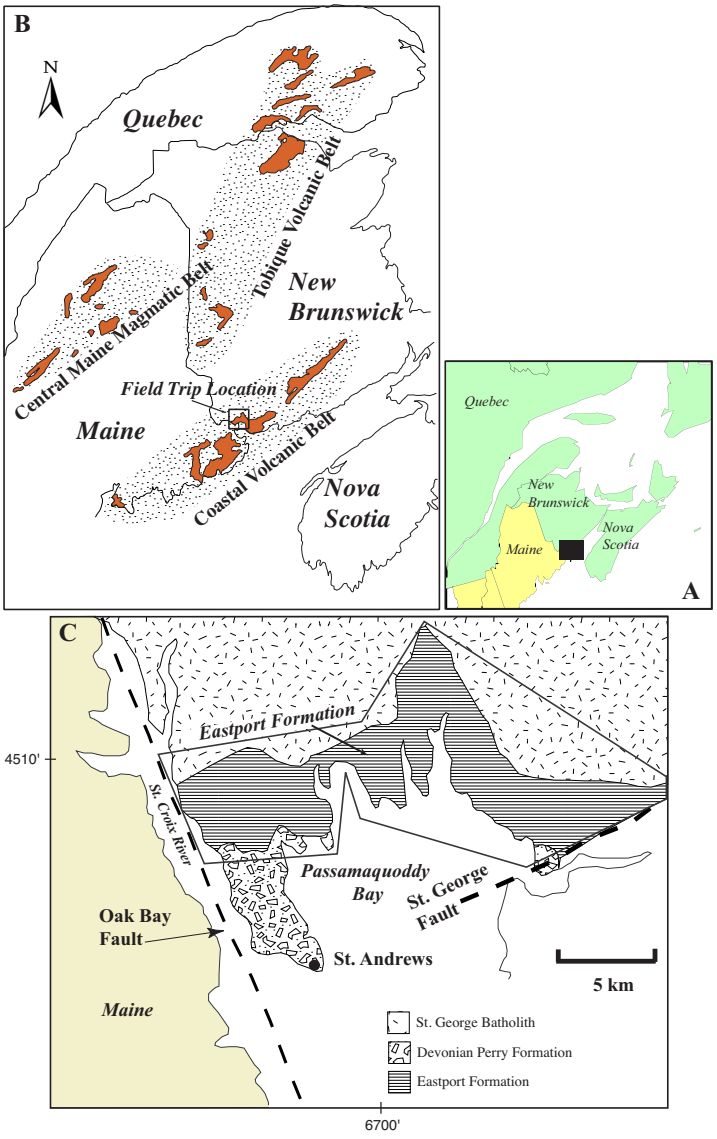

Figure 1. (A) Black box shows the geographic setting of the area. (B) Coastal, Central, and Tobique volcanic belts (after Dostal et al. 1989 and Seaman el al., 2019). Patterned areas show the locations of the belts and dark areas show exposures of volcanic rock. (C) The location of the Eastport Formation in New Brunswick (PBVS, Passamaquoddy Bay Volcanic Sequence) (after Fyffe and Fricker, 1987), detail in Fig. 2.

cyclic nature of the volcanism was controlled by pulses of injection of basaltic magma into the crust triggering large-scale and effusive and explosive felsic eruptions

1 The precise correlation of the Eastport Formation in New Brunswick to its type - section in Maine has not been established. The two units are of the same age and similar geochemistry but the Eastport series (as it was originally called in Maine) is only 2.5 km thick and is separated from the Eastport Formation in New Brunswick by the St. Croix fault.

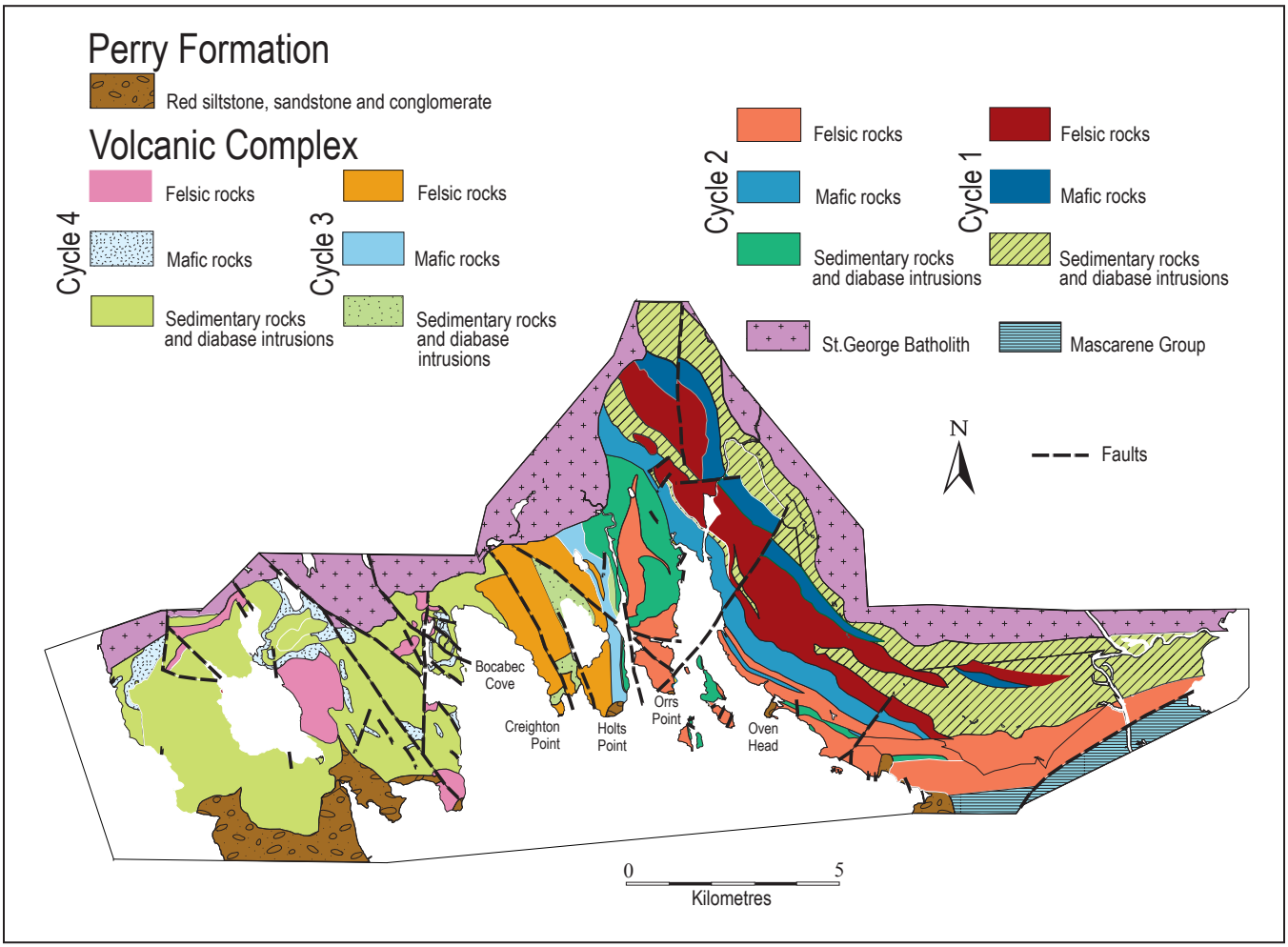

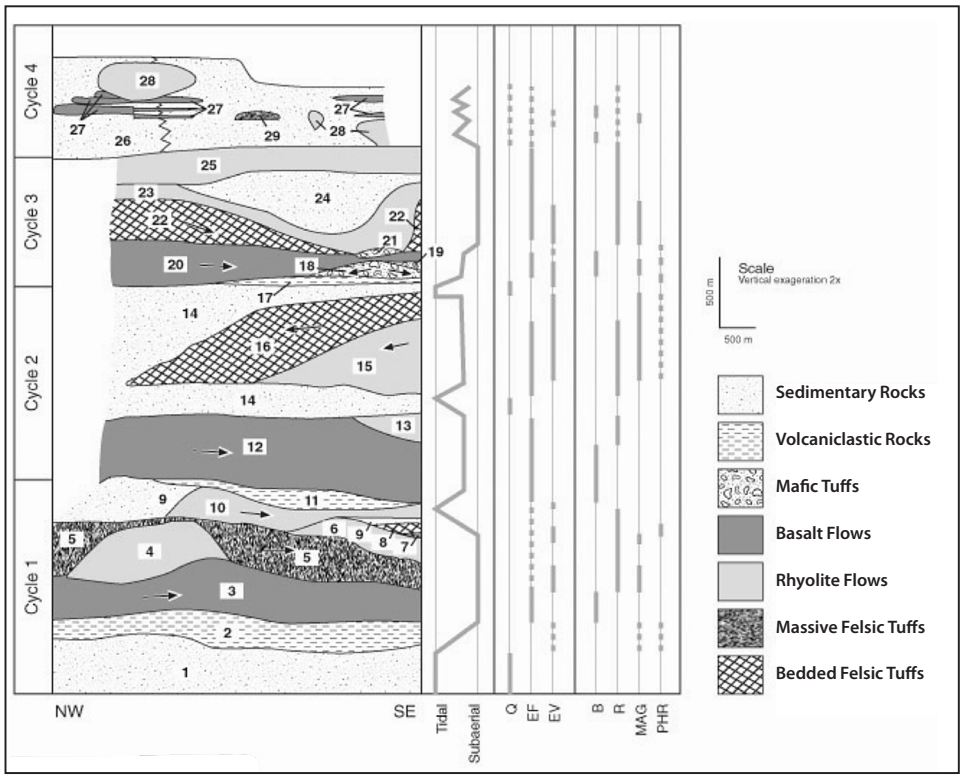

Figure 2. Generalized map of the Passamaquoddy Bay Volcanic Sequence (Eastport Formation in New Brunswick), showing the volcanic cycles; Cycle 1 is the oldest, and Cycle 4 is the youngest (modified after Van Wagoner et al., 2002, 2001).

Figure 3. Generalized conceptional diagram of the Passamaquoddy Bay Sequence (Eastport Formation in New Brunswick). The numbers refer to the order of deposition. Q is quiescence. EF is effusive volcanism, EV is explosive volcanism. B indicates basalt flows. R indicate rhyolite flows. MAG indicates eruptions driven by magmatic volatiles. PHR indicates phreatomagmatic eruptions. From Van Wagoner and Dadd, in prep.

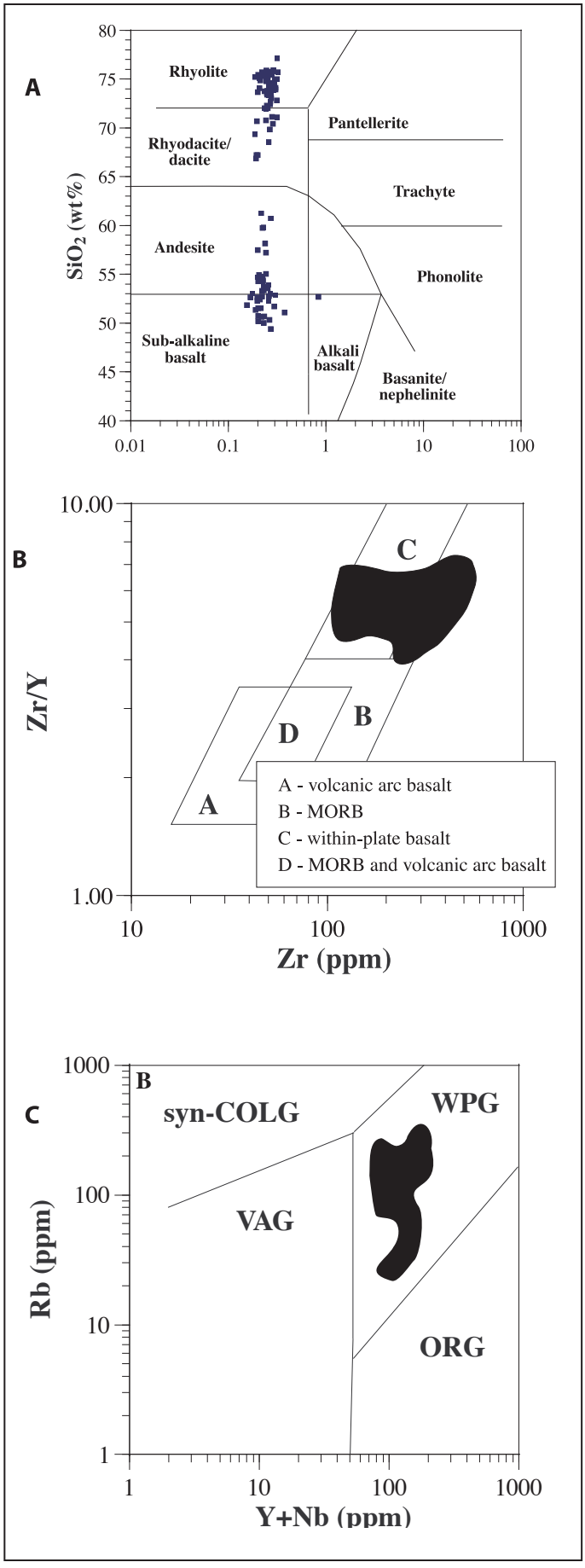

Figure 4. (A) Geochemical classification diagram from Winchester and Floyd (1977) showing that the volcanic rocks of the Passamaquoddy Bay Volcanic sequence are bimodal and subalkaline. Tectonic discrimination plots for (B) the basaltic rocks and (C) the felsic rocks. The black area encompasses the compositions of the rocks analyzed. In both cases, the rocks plot in the within plate field. Diagrams are from (B) Pearce and Norry (1979) and (C) Pearce et al. (1984). ORG - orogenic granites, syn-COLG - syn-collisional granites, VAG - volcanic arc granites, WPG - within palate granites. Modified from Van Wagoner et al. (2002).

(Van Wagoner et al., 2002; Van Wagoner et al., 1994). Intrusive rocks that might be the remnants of the magma chamber for the Eastport, New Brunswick magmatic system have not been specifically identified, as it has for several of the magmatic complexes in Maine. However, plutonic phases of the St. George Batholith are of similar age, geochemistry and tectonic affinity to the Eastport (McLaughlin et al., 2003; Mohammadi et al., 2017, 2019) and are potential candidates.

The age of the Eastport Formation, NB, is based on two dates; 421±3 Ma and an informal age of 423±1 Ma (Mohammadi et al., 2019; Van Wagoner et al., 2003, respectively), which corresponds to the age range of the Coastal Maine bimodal complexes of 424-420 Ma (Seaman et al., 2019, 1995; McLaughlin et al., 2003). Fossil evidence also indicates a similar age (Churchill-Dickson, 2004; Turner and Burrow, 2018).

In contrast, in the northern part of the Tobique Volcanic Belt two age groups of bimodal volcanism are recognized; 422–419 Ma and 417–407 Ma (Wilson et al., 2017). Similarly two age groups also occur in the central part of the Tobique; 422 Ma and 409-405 (Sánchez-Mora, 2021). In the Central Volcanic Belt of Maine, ages for the Traveler Rhyolite (406.3 ± 3.0 Ma, and 407.3 ± 0.5 (Bradley et al., 2000)) and Katahdin pluton (406.9±0.4Ma (Rankin and Tucker, 1995)) correspond to the younger episode of volcanism of the Tobique. This combination of age dates encompass the end of the Silurian Salinic Orogeny (440-423 Ma) and the Late Silurian - Early Devonian Acadian Orogeny (421-400 Ma) (e.g. van Staal and Barr, 2012), and indicates that bimodal volcanism was active from 424 to 407 Ma with a possible hiatus of 2.2 Ma during that period (e.g. Seaman et al., 2019; Wilson et al., 2017).

All three of the bimodal volcanic belts were interpreted to have formed on the Ganderia terrane, which accreted to the eastern margin of Laurentia during

the Silurian Salinic orogeny (e.g. van Staal et al., 2009; Wilson et al., 2017). The geochemical characteristics of the rocks can be explained by volcanism within an intra-arc rift and backarc on the margin of Ganderia/ Laurentia situated above the northwest directed oceanic subducting plate of Avalonia as it approached Ganderia to close the Acadian Seaway (e.g. van Staal and Barr, 2012; van Staal et al., 2014, 2009; Fyffe et al., 1999; Van Wagoner, et al. 2002). However the specific drivers of the extension are uncertain (for a summary see Piñan-Llamas and Hepburn, 2013). More recently, Seaman et al. (2019) proposed a setting similar to the continental intra-arc Taupo rift volcanic zone which is formed by oblique convergence of the subducting margin resulting in extension of the continental crust in the North Island of New Zealand (e.g. Seebeck et al., 2014). Seaman et al. (2019) further suggested that the extension that produced the Coastal Volcanic Belt was followed by flattening of the subducting slab during the Acadian Orogeny (van Staal et al., 2009) to produce the Central Maine and the Tobique volcanic belts. However, age dates for the Tobique suggest that extension related volcanism began at the same time in the Coastal and Tobique belts, but persisted longer, into the Devonian in the Tobique and Central Volcanic Belts. Wilson et al. (2017) proposed an overlap between the Salinic orogeny involving the northwestern part of Ganderia, and the Acadian orogeny involving the southeast, trailing edge of Ganderia which best fits with the age dates.

General Volcanism of the Passamaquoddy Bay Sequence of the Eastport Formation.

The most recent, comprehensive report of the volcanism of the Passamaquoddy Bay Sequence of the Eastport Formation, NB, is by Van Wagoner, et al. (1994). They identified 63 mapable units at the 1:10,000 scale and interpreted the model of eruption and deposition for each unit. This field guide is based largely on that work and theses of Baldwin (1991) and McNeil (1989). Subsequent to producing that report, major construction along Highway 1 produced an abundance of new outcrops. Les Fyffe mapped these sections which improved the accuracy of previous work.

The Passamaquoddy Bay Sequence of the Eastport Formation is 4 km-thick and comprises four cycles of bimodal (basaltic-rhyolitic) volcanism, separated by periods of relative volcanic quiescence represented by shallow water to subaerial sedimentary rocks (Fig. 3). Episodes of mafic-dominated volcanic rocks accompany and typically underlie felsic-dominated sequences in each of the cycles. Sedimentary rocks interfinger with volcanic rocks, but dominantly sedimentary rock sequences are interpreted as times when volcanism was less active. Due to moderate tilting and the shape of the Passamaquoddy Bay coast, which cuts across bedding trends, a nearly complete section through the sequence is exposed, although the lateral extent (and hence volumes) of the units are speculative. Additional impediments to interpreting the volcanic history of the area is that the exposure only reveals a particular transect through the volcanic belt, and more competent units are preferentially preserved, whereas unwelded, fine-grained pyroclastic rocks are more likely to be reworked and eroded. It is also important to keep in mind that this is not layer-cake geology. Volcanic units are notoriously discontinuous. Correlations were based on the most laterally extensive units or packages of units. The sequence is also cut by a number of faults. Nevertheless, the superior exposure provides the opportunity to exam a sequence of volcanic rocks that is part of a large bimodal igneous province.

3.1 Mafic Lava Flows and Peperitic Breccias

Mafic lava flows are exclusively pahoehoe-type sheet flows with undulatory tops, pahoehoe toes, and amygdules that increase in abundance upward within flows. Flow units range in thickness from approximately 12 m to 460 m thick. Individual flows within flow units are 1-12 m thick with oxidized contacts (Fig. 24F). Individual flows in Cycle 4 are thicker overall than those of the lower cycles, but flow units are thinner, being only up 35 m thick. Flows from Cycles 1-3 are thicker and more massive in the north and thin to the south forming pahoehoe toes interbedded with sedimentary rocks.

Most of the flows from the lower three cycles are aphyric or rarely plagioclase-phyric, and have a trachytic or pilotaxitic texture. The thicker flows of Cycle 4 also contain olivine as a phenocryst phase and have an intergranular or subophitic texture (Van Wagoner, et al., 1994).

These flows erupted onto and interacted with wet sediment to form peperitic breccias at the base of the

of some flows in Cycles 1-3 (Fig. 9). These breccias are characterized by clasts up to 0.5 m in size of pillow-like to angular fragments of basalt in fluidized sediment. The jigsaw texture of some of the fractured fragments indicates breakage by quenching and little movement of the clasts (Dadd and Van Wagoner, 2002).

The basaltic flows were interpreted to be more similar to plains-type basaltic lava flows than flood basalts (Van Wagoner et al.,1994), being relatively thin and lacking well-developed columnar joints (e.g. Greeley, 1982; Cas and Wright, 1987). The vent areas were not observed, but variations in thickness of flows in cycles 1-3 suggests that flows originated from a source to the north. The source area in Cycle 4 was not determined.

Mafic Pyroclastic Rocks

Mafic pyroclastic rocks were only observed at two horizons near the base of Cycle 3, and in new exposures along the Basin Road in Cycles 1 and 2. The remnant of a single, monolithic scoria cone has a maximum thickness of about 82 m, and comprises ash- to bomb-sized (≤1 m in length) basaltic scoria fragments, and rare accidental siltstone fragments of the tidal flat siltstones though which the cone erupted. There is no matrix. Some of the bomb-sized ejecta were fluidal when deposited and cemented by agglutination, but the unit is now cemented by secondary calcite. This type of deposit is characteristic of Strombolian-style volcanism (Van Wagoner and others, 1994) (Fig. 24C).

The other two pyroclastic units are vaguely-bedded heterolithic basaltic tuff breccia up to about 35 m thick with beds ranging from 30 cm to 6 m in thickness. Lithic clasts (<60%) of angular to subangular siltstone and gabbro are are up to 1 m, averaging 1-2 cm. Magmatic fragments are amygdaloidal and non-amygdaloidal basalt, some of which are bomb-shaped, and rare cored bombs of lithic ejecta rimmed by basalt. The matrix is non-welded basaltic vitric tuff comprising blocky and bubble-wall glass shards, altered to chlorite. Based on the morphology of shards, and mixture of non-magmatic and magmatic ejecta (Fig. 24D and E). These units were interpreted to be generated by phreatomagmatic eruptions (Van Wagoner and others, 1988; Van Wagoner and others, 1994).

Felsic Pyroclastic Rocks

The felsic pyroclastic rocks are among the most varied and complex rocks in the section because their components, textures and structures depend upon a wide range of parameters including chemical composition of the magma, source and composition of the volatiles driving the eruptions, and all of the physical processes acting to fragment and deposit the ejecta and how they change with time (e.g. Dufek et al., 2015). In addition, deposition is influenced by topography, atmospheric conditions, and distance from vent areas.

Following the terminology in Brown and Andrews (2015), the term, pyroclastic density current, PDC, is used to refer to, "a hot, eruption-derived particulate-gas current that moves laterally along the ground." The term includes pyroclastic flows and surges which are viewed as a continuum of PDC conditions that vary in time and space due to changes at the source and with distance from the source. As such they are considered lithofacies of PDCs. Ignimbrites are a subset of PDCs generated from Plinian and sub-Plinian eruptions. Co-PDC or co-ignimbrite deposits are ashfall deposits from the ash cloud that rises off the top of the PDC and the eruptive plume. These fall deposits represent pauses in PDC activity (Brown and Andrews, 2015). Rocks are named according to the descriptive classification of Schmid (1981).

In the Eastport sequence felsic pyroclastic units comprise a variety of weakly to strongly welded vitric, crystal and lapilli tuffs and tuff breccias. The massive pyroclastic units range in thickness from 40-700 m and the bedded pyroclastic units are from 30 to 534 m thick. Within the bedded pyroclastic units, beds are a few centimeters to 3 m thick. Bedding structures include parallel, cross lamination, and normal and reverse grading of pumice and lithic fragments within beds (Fig. 28A). Flow structures are indicated by stretched pumice and lithic fragments, alignment of crystals, and eutaxitic foliation and ductile folding of the eutaxitic fabric. These ductile folds form in rheomorphic high grade pyroclastic density currents that resemble lava flows (e.g. Brown and Andrews, 2015).

Most of the pyroclastic units include varying percentages of pumice, glass shards, ash, crystals and lithic fragments. Accretionary lapilli and other ash aggregates (e.g. Brown et al., 2010) are components of several of the bedded pyroclastic units (Fig. 10A and 11). Crystals are mostly feldspars and rare euhedral zircon. Hydrous mineral phases are notably absent throughout most of the sequence. Lithic clasts include vesicular basalt, rhyolite and siltstone. Juvenile mafic magmatic lapilli, bombs and cored bombs occur within some of the felsic pyroclastic units indicating synchro-

nous eruption of mafic and felsic compositions.

Matrix material is generally granophyric, recrystallized and devitrified glass. Other features of the densely welded tuffs are spherulites and lithophysae which are formed during relative high temperature devitrification of volcanic glass (Breitkreuz, 2013). The characteristics of these flows are consistent with Plinian and sub-Plinian eruptions.

Felsic Lava Flows and Domes

It can be very difficult to distinguish high grade ignimbrites (those that are deposited above the glass transition temperature) from felsic lava flows. High grade ignimbrites behave like lava flows and dense welding can obscure original pyroclastic textures. Key distinguishing features are basal auto breccias, and steep, lobate and brecciated margins which are common features of rhyolitic lava flows but commonly absent at the base and margins of ignimbrites. The presence of relict glass shards and pumice also help distinguish ignimbrites from lava flows (e.g. Sheikh et al, 2020, and Henry and Wolff, 1992). In this case, autobreccias were observed at the margins of some of the units, but in some cases our interpretations are based on more equivocal evidence.

Felsic lava flows and domes are flow-banded to massive and mostly crystal poor. The units range in thickness from 60 to 435 m and have a variable lateral extent. Flow bands are up to 1 cm thick, planar to undulating, and defined by variations in color (from dark pink to buff), grain size of devitrification microstructures, and size and abundance of fine-grained opaque minerals in the groundmass. The rocks typically have a microgranophyric devitrification texture. Plagioclase and rare sanidine and quartz occur as phenocrysts. Most lava flows contain rare zircon. Primary structures include spherulites, concentrated along flow bands, perlitic cracks near the tops of flows, and autobrecciation at the margins of some units (Figs. 7 and 8).

Columnar joints are well developed within some units. A dome-shaped unit in Cycle 4 is 435 m thick, and has a peperitic breccia at the base and sediment infill breccia (Rosa et al., 2016) at the top (Dadd and Van Wagoner, 2002).

Clastic Sedimentary Rocks: Non-volcanic

The non-volcaniclastic sedimentary rock types of cycles 1, 2 and 4 are dominantly mudstone and fine- to medium-grained sandstone. Minor rock types include conglomerate, and volcaniclastic sandstone. Sedimentary units are up to 900 m thick (thickest in Cycle 4) but are mostly about 200 m thick. Bed thickness ranges from lamination in the finer grained mudstone and sandstone to beds up to several meters thick in the coarser grained sandstone and conglomerate. Sand and silt-sized clasts are predominantly of grains of quartz (40-55%), feldspar (5-15%), primary muscovite (1-5%), and rare pyroxene, detrital zircon, chloritized mafic shards and lithic clasts (0-15%). The framework grains are typically angular to subrounded and elongate to subspherical. Primary sedimentary structures include plane, ripple and herringbone cross-lamination, cross-bedding, dewatering structures, interference and current ripples, mud cracks and rare raindrop imprints. These beds are commonly bioturbated with horizontal and vertical burrows and traces. Fossils include lingulid brachiopods, bivalves, ostracods, and rare gastropods and are indicative of shallow marine in-shore settings (Pickerill and Pajari, 1976; Turner and Burrow, 2018)(Figs. 16C, D and 24A).

Sedimentary rocks of Cycle 3 and also parts of Cycle 4 comprise red conglomerates, sandstones, and mudstones, with features more typical of subaerial, alluvial fan/fluvial deposits. Pebbles and cobbles in the conglomerate are ≤5 cm in length, subangular and include amygdaloidal basalt, diabase, rhyolite, mudstone, siltstone and minor carbonate. Beds are 0.5 cm-1 m thick, and massive, normally graded, current-ripple and ripple-drift cross-laminated and parallel laminated. Other sedimentary structures are current ripple marks, oscillation ripple marks, cut and fill-forming conglomerate channels, mudcracks, shrinkage polygons, raindrop impressions, and rare clast imbrication (Fig. 25). The scour and fill, current-ripple cross-bedding and lamination, and gravel-lag deposits are characteristic of braided channels on an alluvial fan. The massive conglomerate and those with imbricated clasts are probably sheetflood or stream channel deposits.

Volcaniclastic Rocks

The term, volcaniclastic rocks, is used here to refer to sedimentary rocks with a significant component of reworked volcanic clasts. Although units vary in composition, most are derived from mafic sources and comprise basaltic scoria, basalt clasts, altered mafic shards, rare rhyolitic glass shards, and sedimentary rock fragments as well as silicic grains as in the non-volcaniclastic units (Fig. 24B). Less commonly, units comprise

mainly felsic pumiceous clasts. Units range in grain size from mudstone to boulder conglomerate. These beds are poorly sorted, thickly to thinly bedded and are planar to lens shaped. Primary structures include normal and reverse grading, cross-bedding, pebble trails and load structures.

Volcaniclastic units are interpreted to represent reworked mafic and rhyolitic pyroclastic deposits (Van Wagoner and others, 1994). Reworking is indicated by the roundness of basaltic scoria grains, sedimentary matrix, interbedded sedimentary rocks, and sedimentary structures such as channel bedding, cross-bedding, ripple marks, pebble trails and lens-shaped beds. The main volcanic clasts, basaltic scoria and rhyolitic pumice, were probably derived from poorly-consolidated scoria or tuff cones.

Mafic Dikes

The sequence is intruded by numerous dikes of two ages. The Minister's Island Dike is Late Triassic-Early Jurassic, trends roughly east-west, and is related to the opening of the Atlantic (Dunn and Stringer, 1990). Another set of primarily north to northwest trending dikes is related to the Passamaquoody Bay volcanic sequence, being compositionally similar. In many cases field relationships show that these are feeders to the mafic flows. The consistency of their trend was interpreted to reflect the extensional tectonic setting of the volcanism (Van Wagoner et al., 2001).

Summary

The Eastport Formation exposed along the Passamaquoddy Bay Coast is a 4 km thick sequence of basaltic and rhyolitic volcanic rocks and sedimentary rocks. These rocks form the northern extension of the Coastal Volcanic belt. Together with the Tobique and Central Maine volcanic belts, the Eastport Formation is part of a large bimodal igneous province formed in an extensional tectonic setting that was active from the Late Silurian to Early Devonian.

The lower part of the Eastport was intruded by the Saint George Batholith obscuring older portions of the Eastport such that the initiation of bimodal volcanism is unknown. In addition, flow directions, and the lack of clear vent facies for most of the felsic pyroclastic units suggests that the preserved sequence is somewhat distal to the source, and therefore does not represent a maximum thickness nor a complete sequence as the locus of deposition would be expected to change.

The sedimentary rocks indicate deposition in a peritidal environment comprising tidal flats and channels interbedded upward in the sequence with alluvial fan sediments (Cycles 3 and 4), at the margin of a continental landmass (Ganderia) or inland sea. There are periods of relative volcanic quiescence or non-deposition at the particular transect exposed in the Passamaquoddy Bay area, when siliciclastic sedimentation dominates until the final cycle (Cycle 4) which is primarily sedimentary rocks and records the waning stages of volcanism.

Basaltic volcanism typically precedes episodes of rhyolitic volcanism, and the presence of juvenile basaltic ejecta in some of the felsic pyroclastic units is an indication for coeval and co-spatial basaltic and rhyolitic volcanism. Enclaves of mafic rocks in felsic flows and intrusive sequences have been observed elsewhere in large igneous provinces associated with some of the world's largest eruptions (e.g. Bryan et al., 2010; Cimarelli et al., 2008). This relationship is consistent with the injection of mafic magma triggering felsic eruptions (Van Wagoner et al., 2002). The flows, both basaltic and rhyolitic, interacted with wet sediment to form a variety of peperitic breccias (Dadd and Van Wagoner, 2002).

A spectrum of eruptive and depositional styles is represented ranging from the Hawaiian and Strombolian-type volcanism of the basaltic flows and pyroclastic scoria deposits, to highly explosive rhyolitic sub-Plinian to Plinian rhyolitic pyroclastic eruptions forming PDCs and high grade ignimbrites. Basaltic flows are pahoehoe-type flows that had a source in the northern part of the map area. A basaltic scoria cone deposit and evidence for such deposits in the clasts of volcaniclastic units in Cycle 3 represent Surtseyan-type volcanism. This area also includes a significant component of rhyolite flows. This combination of volcanic deposits, particularly the apparently large volume rhyolite lava flows, intensely welded rheomorphic ignimbrites, ash deposits with abundant ash aggregates and accretionary lapilli, and the associated pahoehoe-style basaltic flows were interpreted by Van Wagoner et al. (1988, 1994) to be most akin to Snake River-type volcanism (e.g. Branney et al., 2008; Knott et al., 2016).

Stillwater Road: Cycle 1

Access from Hwy 127 via Reardon Road then north on Stillwater Road. Outcrops are along the west side of the Digdeguash River.
Stop at 45° 12.2207′ N, 66° 57.1865′ W

The Stillwater Road approximately follows the Digdeguash River from its junction with Reardon Road to the intersection with Burns Brook Road to the northeast. In this area the Digdeguash River cuts through (from northeast to southwest) the St. George Batholith, the lowermost sedimentary rocks in the area and a sequence of interbedded tuffs, volcaniclastic, and sedimentary rocks. This stop is within a sequence of the heterolithic lapilli-tuffs, and tuffaceous sediments. The most distinctive bed is a pumice-rich heterolithic lapilli tuff interbedded with a finely laminated tuffaceous siltstone that exhibits soft-sediment deformation features (mostly visible in thin section) (Fig. 5). Following the river to the north, textures and structures remain well preserved but the rocks have been metamorphosed by the St. George Batholith (Fig. 5).

Though this is the oldest volcanic unit mapped, it does not represent the initiation of volcanism, which is obscured by intrusion of the batholith.

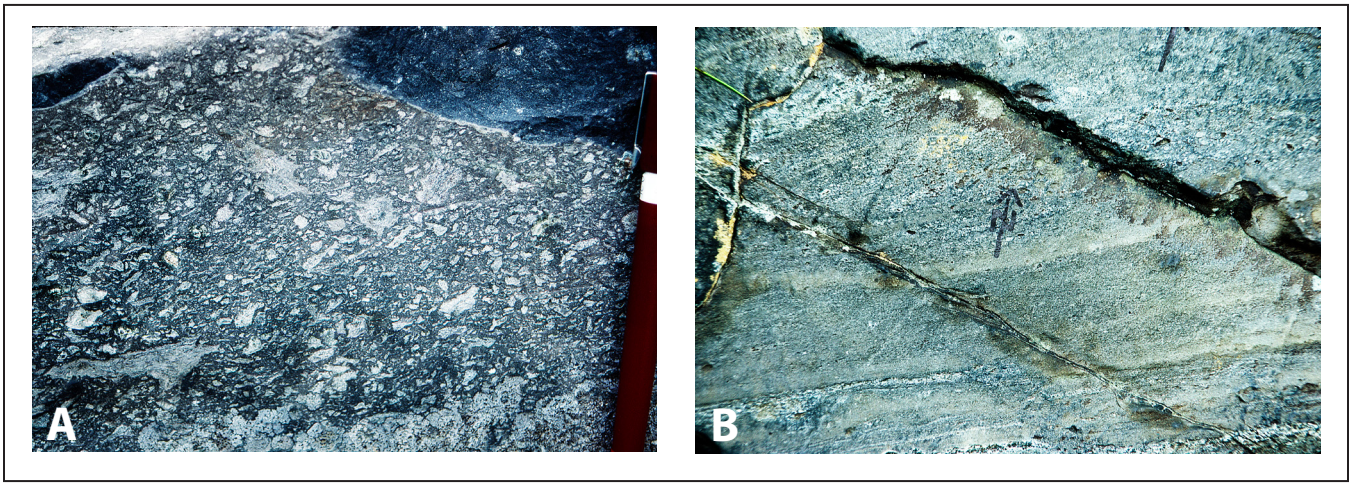

Figure 5. (A) Lapilli tufff with clasts of wispy-shaped pumice. Photo K. Dadd**. (B) Interbedded volcaniclastic mafic siltstone with current ripples. Shards and pumice are visible in thin section.** Photo W. McNeil**.**

Reardon Road: Cycle 1

Stop 1. Reardon Road. Contact between felsic flow and underlying tuff
North side of Reardon Road, about 100 m northwest of Stillwater Road. 45° 11.7113′ N, 66° 57.6468′ W

Excellent exposure of the contact between a basaltic lapilli tuff of Cycle 1 (dark grey rocks below the top of the measuring stick) and the rhyolite flow of Cycle 1. The measuring stick is 1 m in length. The contact, and much of felsic flow is a relict glass with a patchwork of microspherulites (Fig. 6).

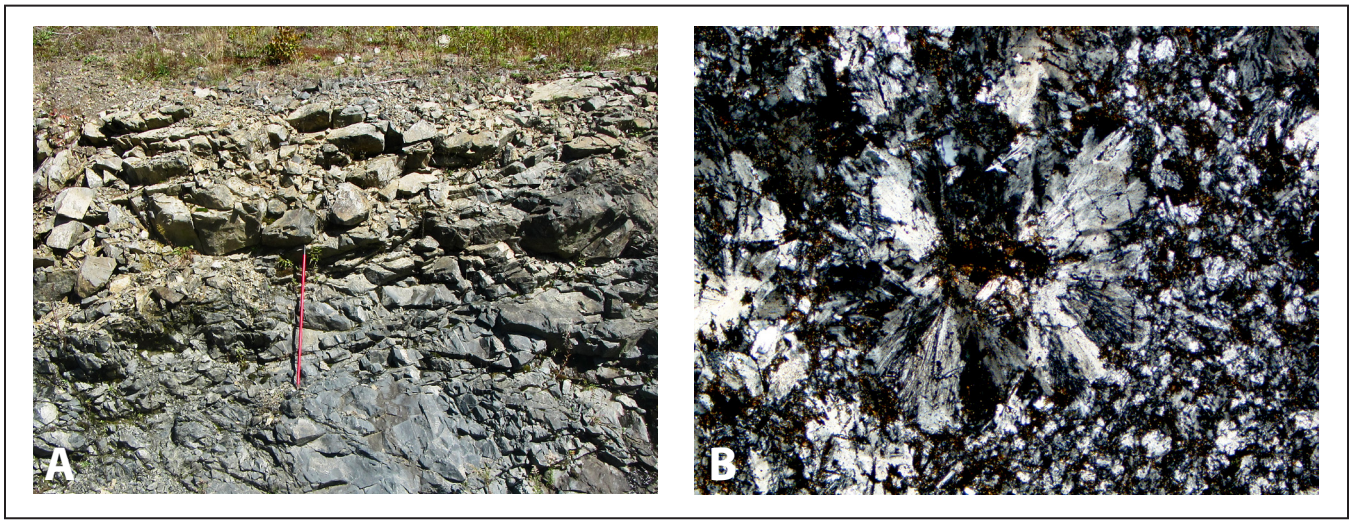

Figure 6. (A) Contact between felsic flow of Cycle 1 and underlying tuff. Photo L. Fyffe**. (B) Vitrophyric base of the felsic flow. 5x, PPL, width of view is 2.2 mm.** Sample M. Thicke. Photo N. Van Wagoner.

Stop 2. Reardon Road. Banded felsic flow with brecciated margin.
Reardon Road just north of Basin Road. 45° 11.9686′ N, 66° 57.9405′ W

Safety Warning. These rocks are slippery and the rock face is steep. Please stay off the rocks.

The same rhyolite as the previous location showing banding and brecciation at the margin. This was interpreted to be a peperitic breccia formed by interaction with wet sediments. Autobreccias are also a common feature of flows and domes which are distinguished from pepperites by being clast supported with in-fill sediment (Rosa et al., 2016). The flow banding is defined by changes in colour and abundance of dendritic or swallowtail crystallites which are aligned to form a trachytic texture. This unit is trachytic in composition. While it can be difficult to distinguish silicic lava flows from strongly welded rheomorphic ignimbrites, the crystal morphology and texture is indicative of rapid crystallization from a melt (eg. Henry and Wolff, 1992), as opposed to a devitrification texture (Fig. 7).

Figure 7. Reardon Road banded and brecciated rhyolite flow. (A) This flow banded rhyolite is the lowermost felsic unit in the map area. (B) Flow margin breecciation. Photos A and B: L. Fyffe. **(C) Flow banding and crystallites of plagioclase. 5x, PPL, width of view is 2.2 mm.** Sample M. Thicke, photo N. Van Wagoner.

Barker Road: Rhyolite Flow and Autobreccia, Cycles 1 and 2

Access via Barker Road from Hwy 1.

This roadcut is a good place to examine the textures of a rhyolite flow and associated breccia. Distinguishing between rhyolitic lava flows and rheomorphic ignimbrites is not always straight forward (e.g., Henry and Wolff 1992; Branney et al., 2008; Sheikh et al., 2020; Naik et al., 2021). Features such as absence of shards, pumice, and broken pyrogenic crystals are considered to be equivocal because they can be masked by the high temperatures and flow of rheomorphic tuffs (Henry and Wolff, 1992). The occurrence or absence of spherulites and lithophysae is also not diagnostic as they are common features of both welded ignimbrites and rhyolite-dacite lava flows. However, basal breccias seem to be a diagnostic features of lava flows. (e.g. Sheikh et al., 2020 Henry and Wolff, 1992).

Stop 1: Cycle 1

45° 10.3106′ N, 66° 56.8136′ W

The rhyolite at this stop is very sparsely alkali-feldspar phyric (no quartz or hydrous phenocrysts), and the ground mass is granophyric. Flow banding is well-developed and the crystals that do occur are not broken. The unit does contain rare juvenile lapilli and spherulites in places. The breccia at this stop was interpreted to be an autobreccia (McNeil, 1989) (Fig. 8).

Considering the cycles of volcanism, it might be noted that this flow is along strike with a flow and associated breccia exposed on the Basin Road. However, the two are mapped as a separate units because they are separated by a thin, but mapable bed of sedimentary rocks. The two flows are chemically similar.

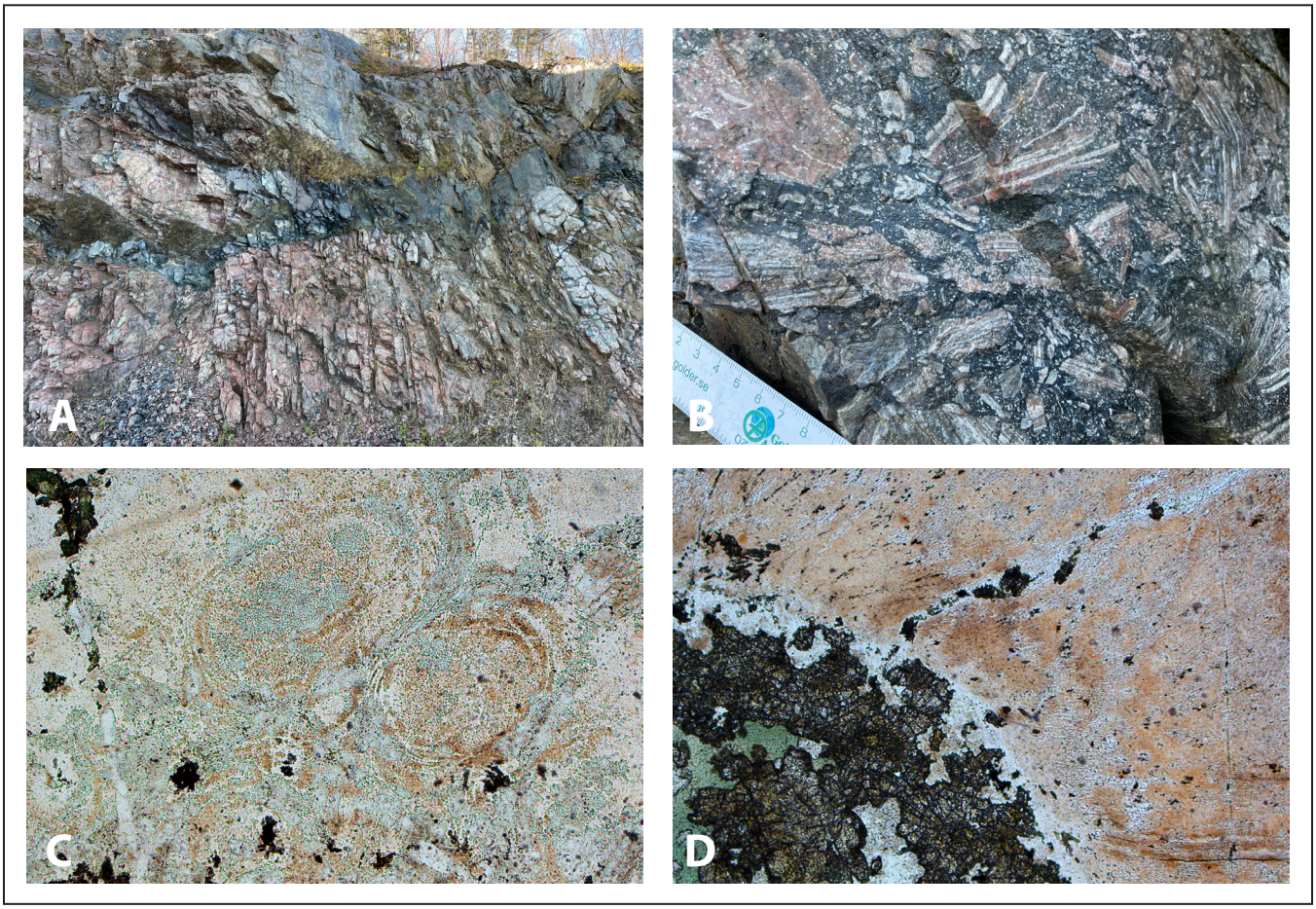

Figure 8. The Barker Road Rhyolite: (A) Outcrop photo showing an intense zone of brecciation on the right. (B) Close up of the breccia showing the range of sizes and textures of the clasts. Photos S. Van Wagoner
(C) Perlitic cracks in a flow band of rhyolite. (D) Margin of large spherulite. The core is altered to epidote and chlorite. Both images at 5X, PL, Width of field is 2.2 mm. Sample W. McNeil. Photos N. Van Wagoner

Stop 2: Cycle 2. Barker Road at the Broken Bridge, Peperitic Breccias of Mafic flows

45° 10.6687′ N, 66° 57.5061′ W

Peperitic breccia or "peperite" is a texture formed by the mingling of magma or lava with wet sediment. Peperites are a common feature of the Passamaquoddy Bay volcanic sequence, because voluminous volcanism was accompanied by peritidal sedimentation (Fig. 3). Peperites of the area are associated with both the basaltic and rhyolitic lavas and magmas, but basaltic peperites tend to have a fluidal textures, and rhyolitic peperites tend to be of the blocky variety (Dadd and Van Wagoner, 2002). At this stop basaltic peperites are exposed in glacially polished outcrops. They formed when pahoehoe-type mafic flows flowed over and bulldozed into wet, underlying unconsolidated silt and mud (Fig. 9).

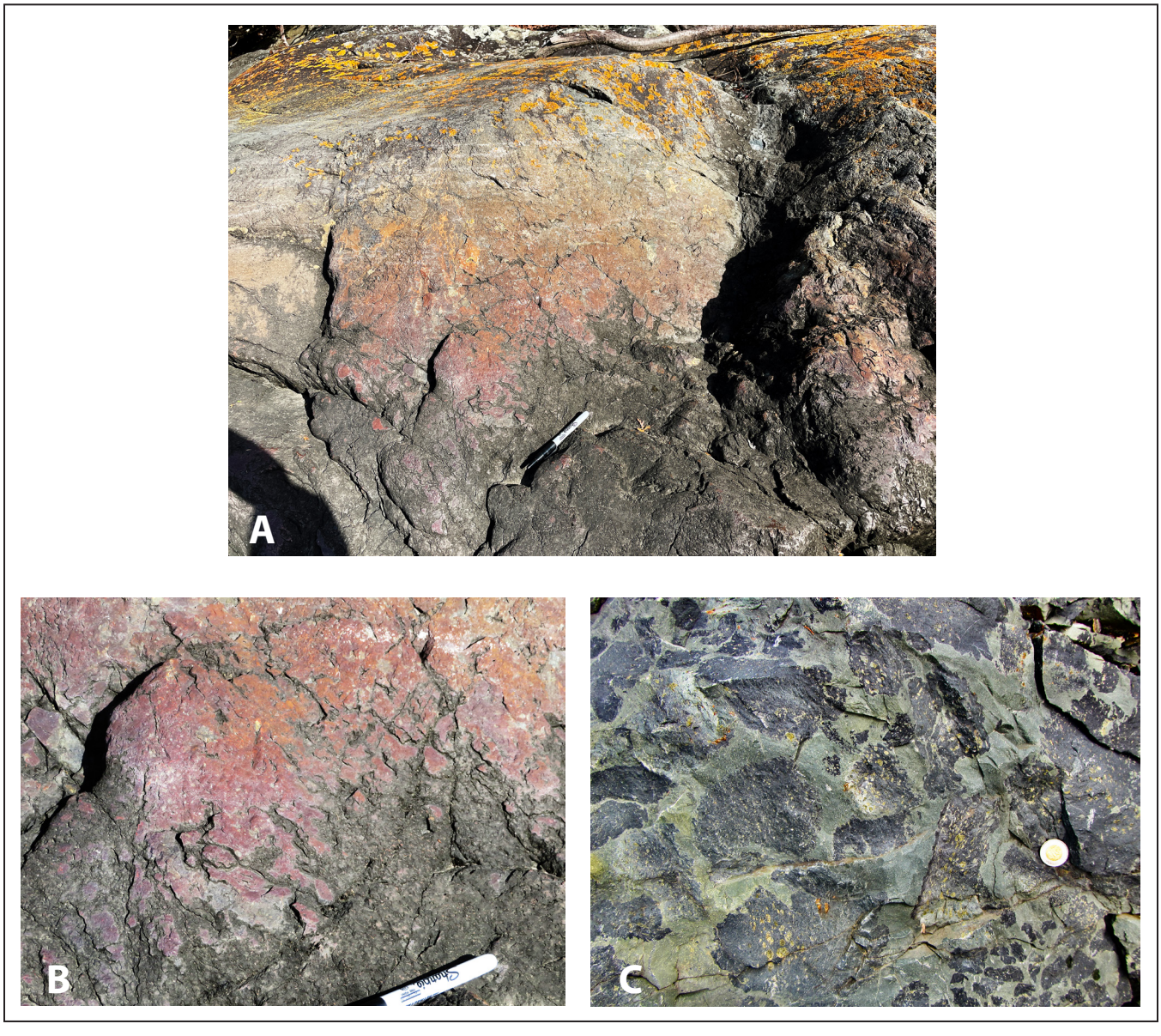

Figure 9. Basalt peperite. (A) This outcrop shows bud-like forms of basalt in the underlying sediment. (B) Detail of (A). (C) Outcrop photo of the same unit exposed in a road cut of highway 1. The peperitic breccia consists of dark grey amygdaloidal basalt fragments of a basalt flow of Cycle 2, in a matrix of olive-green mudstone. Toonie for scale. Photo A: S. Van Wagoner, B: N. Van Wagoner, and C: L. Fyffe.

Oven Head Tombolo and Cove: Cycle 2, Rhyolitic Pyroclastic Density Currents

Access via the Oven Head Rd. (located just before "Ossie's Lunch") off Rd 760. 45.1419023, -66.9327632

Stop 1. Accretionary lapilli and ignimbrite and co-ignimbrite deposits

The tombolo is up section from the rocks exposed in the cove which are stops 2 and 3 at this locality. After visiting the tombolo continue to the north and observe the cliff outcrops in the cove.

Tombolo Section. The main part of the tombolo comprises red sedimentary rocks of the Devonian Perry Formation and the unconformity surface is exposed on the headland. The Silurian volcanic rocks at this stop include tuff, lapilli tuff and accretionary lapilli tuff of Cycle 2 and these are some of the best exposed accretionary lapilli tuff sequences in the area (Figs. 10-12).

The tuff and lapilli tuff units comprise rhyolitic pumice and rhyolitic lithic fragments in a fine-ash matrix. Clasts are angular to subangular and structures include normal, reverse and symmetrical grading, ripple cross-stratification, and lenticular bedding. The components of the accretionary lapilli tuff lenses are accretionary lapilli, pumice, and feldspar crystals of varying proportions in a matrix of platy and tricuspate glass shards and fine to coarse ash. The accretionary lapilli are 3 mm-2.5 cm, rounded to slightly flattened and concentrically zoned. In some beds the accretionary lapilli are both whole and broken (Fig. 11). Beds are 1-15 cm thick and defined by variation in grain size, color and concentrations of accretionary lapilli. Fine internal laminations are generally planar, although locally there is large-scale cross-bedding and mega ripples (wave height 40 cm, wavelength 1.5 m), and normal, symmetric and reverse grading (Fig. 10). In addition to accretionary lapilli tuff, some beds contain other ash pellets which are structureless to weakly concentric aggregates, and cored pellets, comprising a lithic clast coated with an aggregate of fine ash. The terminology for ash aggregates is from Brown et al (2010, Table 1).

A note about accretionary lapilli: Accretionary lapilli are approximately spherical aggregates of ash with a concentric structure (e.g. Moore and Peck, 1962), and are one of a variety of morphologies of ash aggregates (e.g. Brown et al., 2010; Schumacher and Schmincke, 1991). They occur in pyroclastic flow, surge and fall deposits, and are commonly associated with phreatomagmatic eruptions (e.g. Gençalio-lu-Kuşcu et al., 2007; White and Valentine, 2016). The absence of accretionary lapilli or blocky shards cannot be used as criteria to rule out the possibility that a deposit was formed by phreatomagmatic processes, nor are accretionary lapilli diagnostic of this process (e.g. White and Valentine, 2016; Brown et al., 2010).

It was once assumed that accretionary lapilli formed exclusively in the eruption column. Tomita et al. (1985) studied accretionary lapilli from the May 22, 1983 eruption of the Sakurajime volcano, and identified gypsum crystals in spherical spaces between ash particles, leading to the interpretation that fine ash became wet in the rising eruptive cloud due to condensation of moisture derived from the vent during conditions of high humidity, allowing the particles to stick together and then become cemented with the precipitation of secondary minerals. Their observations were subsequently supported by the wind tunnel experiments of Gilbert and Lane (1994), who reproduced the formation of accretionary lapilli in the presence of hygroscope acid solutions. The microphysical parameters that influence aggregation in eruption clouds were further quantified by Textor et al. (2006a, b) through numerical experiments using a plume model. Subsequently, Mueller et al. (2016) used fluidized bed experiments to simulate and numerically model conditions within eruption plumes and pyroclastic density currents, to demonstrate that the production of stable ash aggregates is possible in both environments given relatively high (but volcanically reasonable) amounts of NaCl.

Field observations from pyroclastic couplets (paired ignimbrite and co-ignimbrite deposits) at Tenerife showed the absence of accretionary lapilli beyond the extent of the ignimbrites, supporting the growth of accretionary lapilli in the ignimbrite rather than the plume (Brown et al., 2010). They found that in bed forms and thickness similar to the exposures at Oven Head, ash pellets were more typically associated with airfall deposits while accretionary lapilli were exclusive to deposits of the density currents.

Outcrop Description Detail

Thick-ness	Bed	Description
100 cm	K	Laminated and cross laminated lapilli tuff with pumice and ash pellets, very similar to G. Matrix is ash and platy and cuspate shards.
140 cm	J	Bedded lapilli and ash-pellet lapilli that are less than 1cm, and commonly less than 0.5 cm (accretionary lapilli were not observed in thin section). Pumice (2-4 mm thick and up to 2 cm long) shows no preferred orientation. Ash pellets are concentrated in beds and lenses where they are up to 60-95% Most of the exposure is a bedding surface.
137 cm	I	Accretionary lapilli tuff. Poorly exposed laminated and bedded lapilli tuff and accretionary lapilli tuff similar to A and G. Lapilli are 50-60%, almost all are flatted parallel to bedded. Broken lapilli are in the matrix. The largest accretionary lapilli (5 cm) are formed by an agglutination of several lapilli that are surrounded by a rim of ash. Fig. 11.
140 cm	H	Massive coarse ash lapilli tuff with 20% cored accretionary lapilli and ash pellets, round and also stretched parallel to flow, and pink flattened pumice, in a matrix of coarse flattened cuspate and platy shards and ash indicating moderate welding. Figs. 10 and 12.
228 cm	F/G	Accretionary lapilli tuff, with 3% pumice fragments similar to B and D, but with larger lapilli, 1-2.5 cm. Accretionary lapilli are concentrated in lenses 5-15 cm thick where they are up to 60% of the beds, in a coarse-ash matrix. Some lapilli are broken forming part of the matrix. Accretionary lapilli lenses are about 30%, laminated beds are 20%, and the remainder of the bed is massive. Figs. 10 and 11.
25 cm	E	Laminated tuff similar to C, poorly exposed
5 cm	D	Accretionary lapilli tuff. Same as bed B but not graded. Pumice are about 5%, 1-3 mm thick, and flattened, up to 5 cm long. TS 6N-46D
13 cm	C	Tuff. Beds are lens-shaped, 3mm – 3 cm thick. Thicker beds (> 0.5 cm) are massive or normally graded, fine green-grey. Thinner beds contain up to 50% pink, flattened pumice (< 1mm thick and up to 1 cm long). Lenses are up to 20 cm long and distinctly finely laminated and cross laminated. This bed grades upward over the top 0.5 cm, by the addition of accretionary lapilli, to the next bed. Figs. 10 and 11, TS 6N-46C
20 cm	B	Accretionary lapilli tuff, contains 30% round (occasionally oval and elongate parallel to bedding), concentrically zoned accretionary lapilli, up to 1.5 cm in diameter, with largest lapilli concentrated near the centre forming a symmetrically graded bed. Other lapilli are 1% fine-grained pink rhyolite, 1 mm to 1 cm with long axis parallel to bedding. Matrix is dark, green-gray, fine ash.

65 cm	A	Vaguely bedded and laminated heterolithic lapilli tuff. Bedding is defined by changes in the size and abundance of lapilli. Lapilli are mostly aphyric and feldspar-phyric blocky rhyolite clasts, and pumice, showing vague and inconsistent alignment. Crystals are feldspar up to 4 mm in size. Vague reverse grading in lower in 3 sets about 15 cm thick, upper layer is normally graded by loss of lapilli. Matrix is unwelded and contains shards with platy and cuspate shapes. Fig. 12.
± 3 m		Poorly exposed on iron-stained surface of beach cliff

Figure 10. (A) Lenses of accretionary lapilli in Bed F. (B) Large flattened pumice from Bed H just above scale. (C) Laminated bedding in Bed C showing flattened pumice and alignment of rhyolite lithics and feldspar crystals. Photos N. Van Wagoner

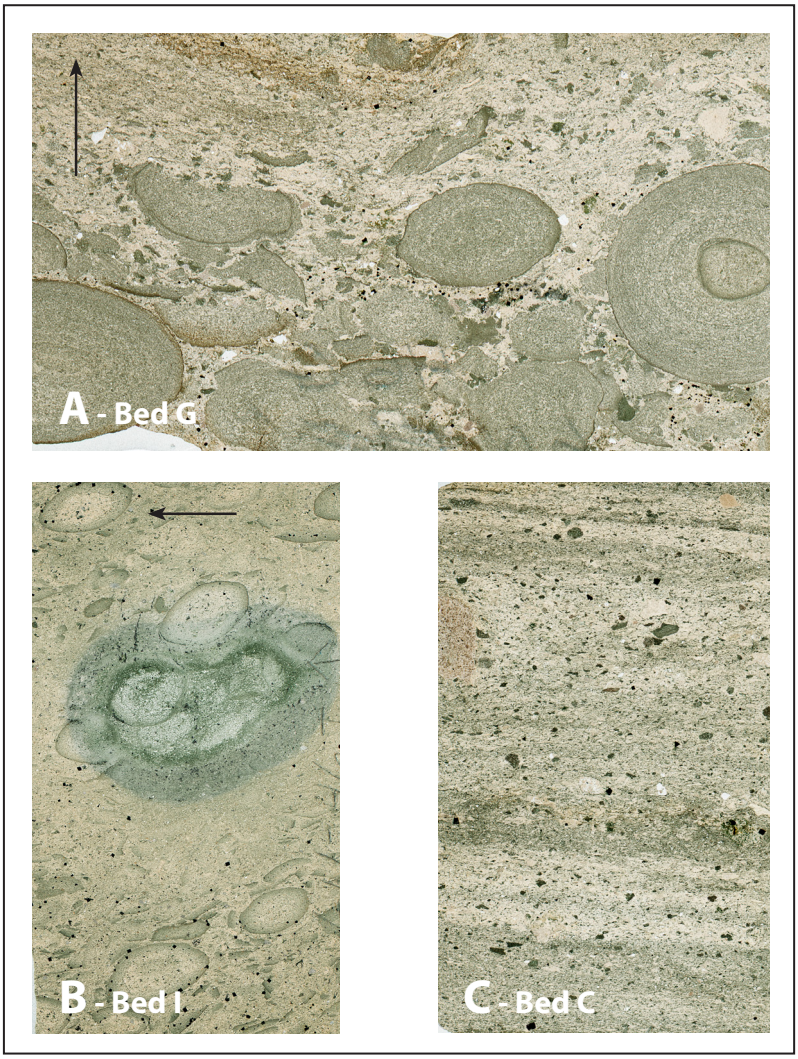

Figure 11 (left). Thin section slide scans. (A) Bed G showing concentric round and broken accretionary lapilli. (B) Bed I showing 3 layers. The upper and lower layers are accretionary lapilli-rich but the lapilli are more deformed and fragmented in comparison to Bed G and the lack the same fine zonation. The fragment in the middle of the the slide is an aggregate of accretionary lapilli surrounded by an alteration halo. (C) Laminated bedding from Bed C.

Figure 12 (below). Photomicrographs from Beds A (bottom of sequence), and H (at the top). (A) The large fragment filling the middle of the image is a basalt lapilli. (B) Bubble wall, blocky and platy shards in a fine ash matrix. The fragment at the bottom of the slide is an ash aggregate. (C) Cored pellet above a deformed shard. Note other ash pellets on the right side of the thin section. (D) Deformed cuspate and platy shards. All photos are at 5x, PPL, width of view is 2.2 mm. Photos N. Van Wagoner

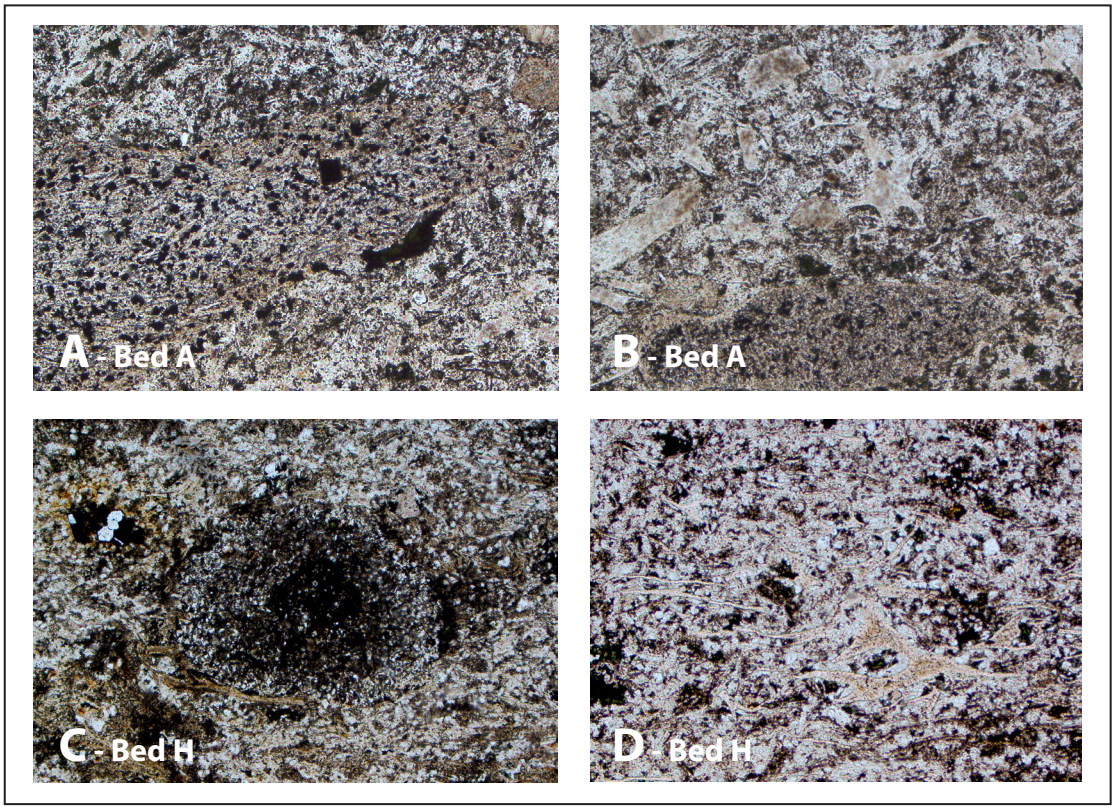

Stop 2. Hydrothermally altered pyroclastic flow

45° 8.8031' N, 66° 56.3106' W

At this stop a greenish lithic crystal tuff is in contact with a hydrothermally altered and brecciated rhyolitic rheomorphic flow, accentuating the flow banding. The tuff contains crystals of feldspar and flattened pumice mostly 2 cm but up to 20 cm long (Fig. 13).

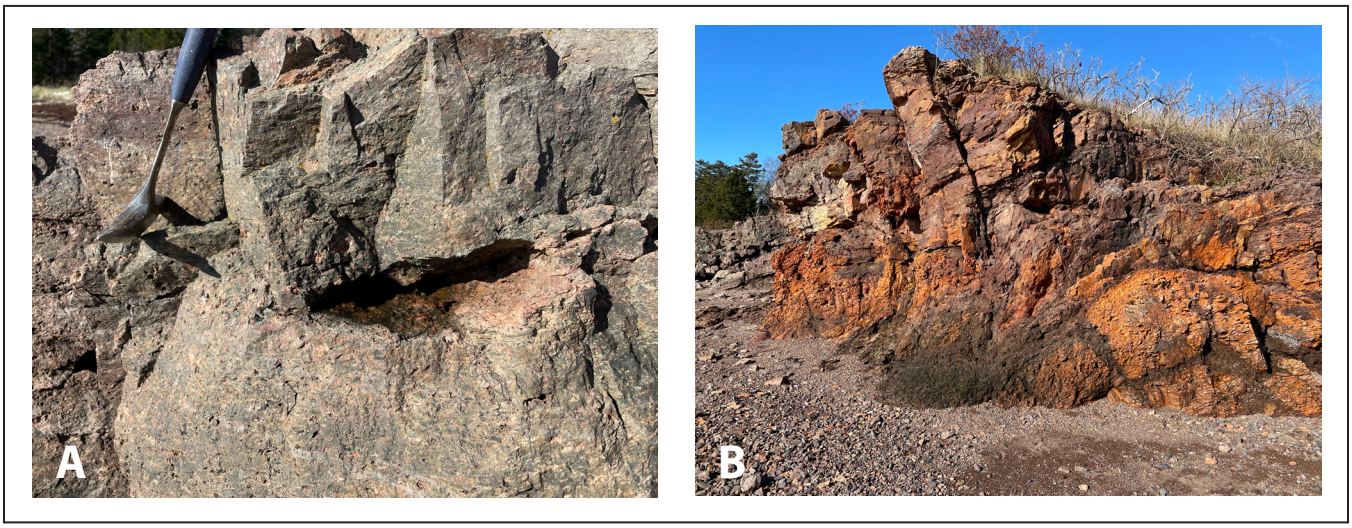

Figure 13. (A) Lithic-crystal tuff. (B) Altered and brecciated rhyolite. Photos by S. Van Wagoner.

Stop 3. Heterolithic tuff to tuff breccia

45° 8.8145' N, 66° 56.1093' W

This heterolithic lapilli tuff to tuff breccia contains up to about 30% lapilli, blocks and bombs, in a matrix of welded shards and stretched and welded pumice forming a banded eutaxitic texture in places. The unit is poorly sorted and matrix supported. The larger juvenile lapilli and bombs are both vesicular to scoriaceous basalt and rhyolite with magmatic textures. Some of the bombs are cored bombs, rimmed by basaltic lava. Banding is very fine, on the mm scale, and folded in places suggesting rheomorphism. The size of the pyroclasts suggests a near vent facies. The combination of both mafic and felsic juvenile pyroclasts suggests coeval and co-spatial pyroclastic basaltic and rhyolitic pyroclastic volcanism. McNeil (1987) interpreted this facies to represent a near fall and PDC deposit from a magmatic sub-Plinian to Plinian eruption.

While it is not common to find mafic juvenile pyroclasts in a felsic PDC it is a rather regular feature in the Passamaquoddy Bay sequence. In a study of the largest eruptions on Earth, Bryan et al. (2010) documented a similar occurrence of juvenile mafic pyroclasts in welded ignimbrites from the Karoo Large Igneous Province, and the Whitsunday silicic Large Igneous Province, Cid Island, Australia, which they attributed to simultaneous eruptions of basalt and rhyolite (Figs. 5 and 6).

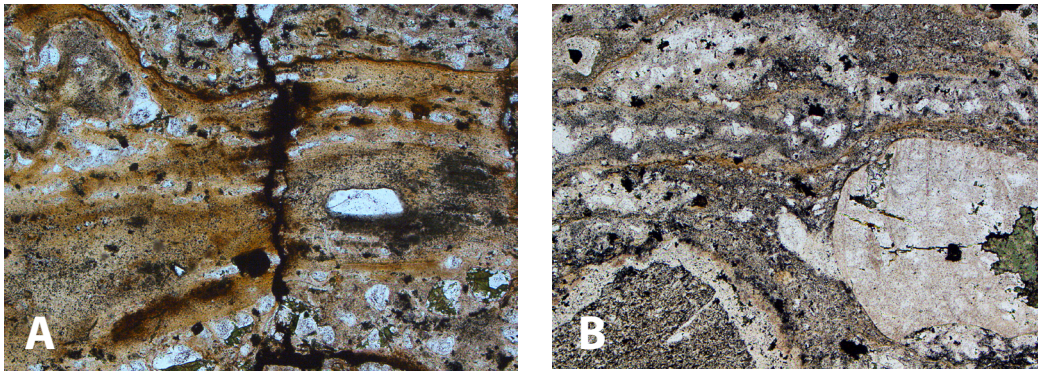

Figure 14. Heterolithic, welded pyroclastic flow and flow breccia exhibiting a eutaxitic texture formed by stretching of shards and pumice that drapes lithic fragments. Note the accidental lithic fragment on the lower left of (B) is rimmed by lava. 5x, PPL, width of field is 2.2 mm. Samples W. McNeil. Photos N. Van Wagoner.

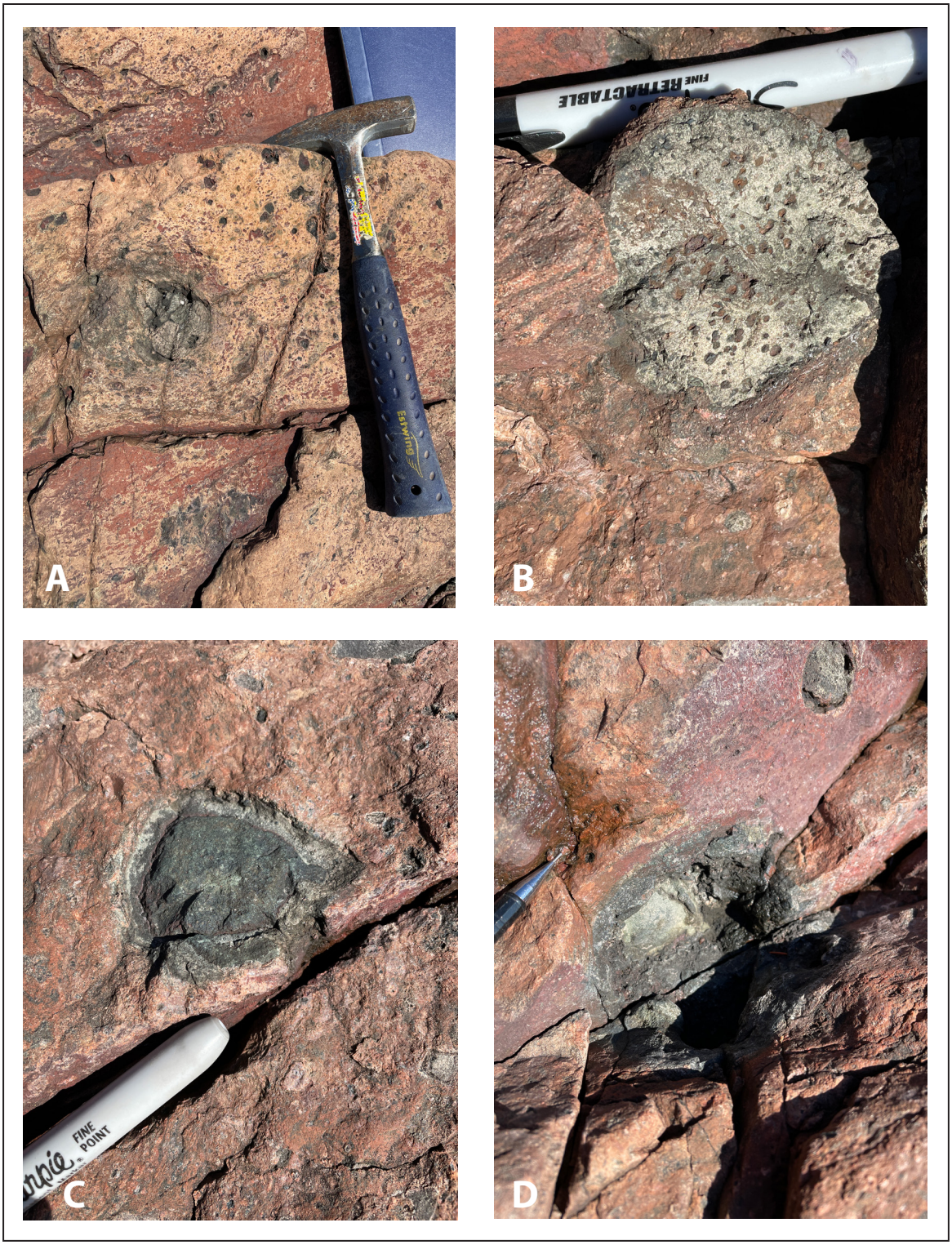

Figure 15. Juvenile mafic pyroclasts in a rhyolitic welded lapilli tuff and tuff breccia. (A) Two mafic lapilli are to the left of the hammer. (B) Large basalt lapilli with a round shape and delicate protrusions indicating that the fragment is magmatic. (C) and (D) are cored bombs. Photos S. Van Wagoner

Basin Road to Basin Access Road: A Traverse Though Cycles 1 and 2

Stop 1. Cycle 1. Maroon Sedimentary Rocks.
Basin Road from Hwy. 127, about 500 m northwest of Reardon Road. 45° 12.0248 N -66° 58.3407 W

This southwest dipping sequence of thin- to thick-bedded maroon, fine-grained sandstone and siltstone of Cycle 1 is stratigraphically above the peperitic rhyolite described on Reardon Road. There is abundant evidence of soft-sediment deformation including load structure, micro ball and pillow structures, and small slump folds. The conformable contact between these maroon sediments and the overlying mafic tuff is sharp (Fig. 16).

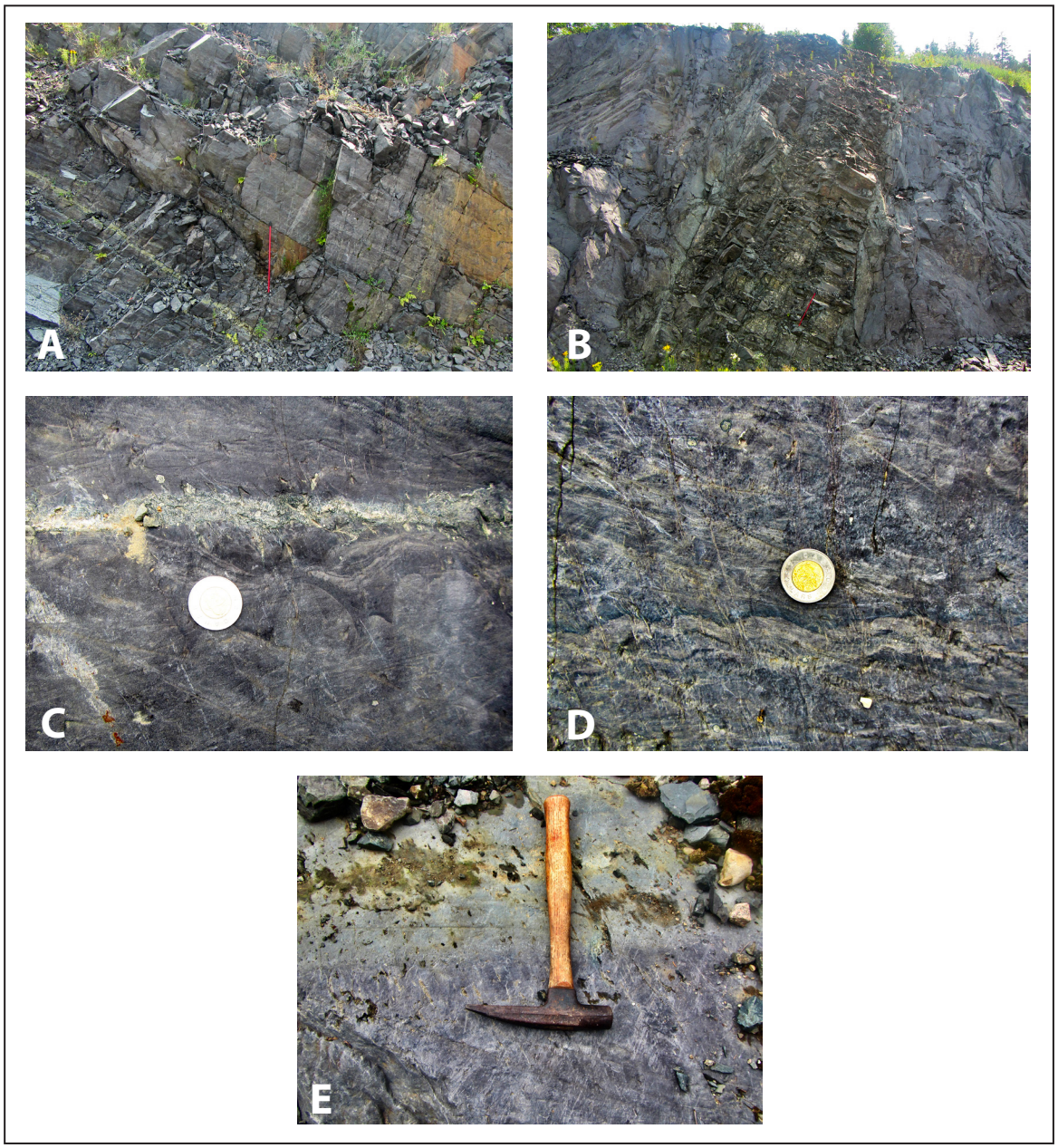

Figure 16. (A) Outcrop photo of bedded maroon sediments. Note the 5 cm thick, green, epidote-rich layer to the left of measuring stick. (B) Diabasic dike in maroon sediments. (C) Load structures. (D) slump folds, (E) Sharp contact between the maroon sediments of Cycle 1 and the overlying mafic tuff. The red measuring stick in photos (A) and (B) is 1 m long. Photos L. Fyffe.

Stop 2. Cycle 1 Rhyolitic Peperite
45° N 11.8814′ N -66° 58.543′ W

This stop is located about 400 m to the southwest of the previous stop and on the southeastern side of Basin Road. The margin of this rhyolitic lava of Cycle 1 has interacted with wet sediment to form a peperitic breccia, a feature very common in the Passamaquoody Bay sequence of the Eastport. The lithophysae attest to the originally glassy nature of the margin of this flow. At this location the rhyolite is also intruded by a fine-grained diabasic dike (Fig. 17).

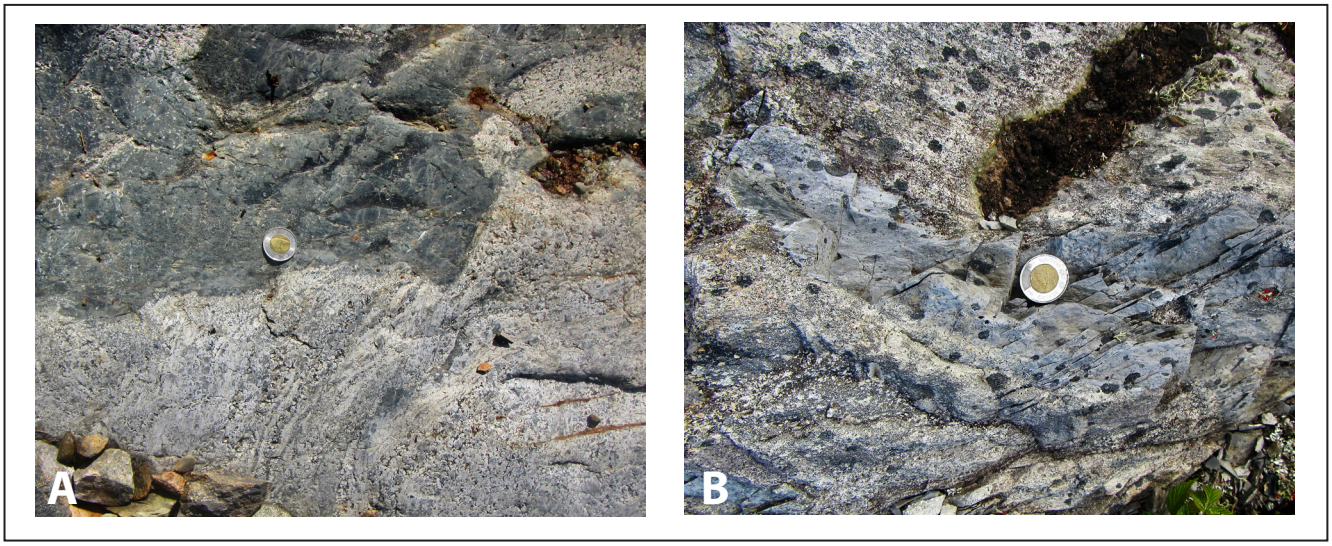

Figure 17. (A) Peperitic texture formed by the interaction of rhyolite lava with wet unconsolidated sediments. Lithophysae follow the flow foliation in rhyolite. (B) One of the of many elongated dark grey sedimentary fragments is pictured in central part of photograph. Toonie for scale. Photos L. Fyffe

Stop 3. Cycle 2. Basaltic bedded lapilli tuff
45° 11.8561′ N -66° 58.5898 W to 45° 11.843′ N -66° 58.5784′ W

About 100 m south of the Stop 2 on the west side of the Basin Road. These mafic lapilli tuffs overlie the maroon sediments and include beds of maroon sediment that have a significant component of volcanic (mostly basaltic) clasts (volcaniclastic beds). Beds are massive, laminated and cross laminated, and graded (Fig. 18).

Stop 4. Cycle 2. Amygdaloidal Basalt and contact with Cycle 3
45° 11.7067′ N -66° 58.5456′ W to 45° 11.7737′ N -66° 58.5705′W

Continue about 250 m south of the previous stop to an outcrop on the west side of the road. This outcrop is a good example of the mafic flow sequence at the start of Cycle 1. These flows are part of the same unit as the flows and peperitic breccias that are exposed in outcrops at the western end of Barker Road (Fig. 9). The flows are dark grey and contain large amygdules typical of subaerial flows and typical of most of the mafic flows in this sequence. The uppermost part of this sequence is in fault contact with the overlying maroon sediments of Cycle 3 (Fig. 19).

Figure 18. (A) Distinctly bedded, dark grey, basaltic lapilli tuff from Cycle 2 is exposed in a large roadcut on the western side of the Basin Road immediately south of the low-lying outcrop of maroon sedimentary rocks that marks the top of Cycle 1. A 15 cm-thick diabasic sill intrudes the section. The unit is thin-bedded (8 cm) to thick-bedded (50 cm). 1 m measuring stick for scale. (B) Thick bed of basaltic lapilli tuff in Cycle 2, exposed near the top of the outcrop on the western side of the Basin Road. The unit is graded and lapilli are angular in shape. Pink felsic pyroclasts occur locally. Dark grey pyroclasts to the far right of hammer head may be scoria fragments. (C) Beds of the mafic lapilli tuff in the roadcut on the western side of the Basin Road are thin-bedded, normally graded and cross bedded. Loonie for scale. Photos L. Fyffe.

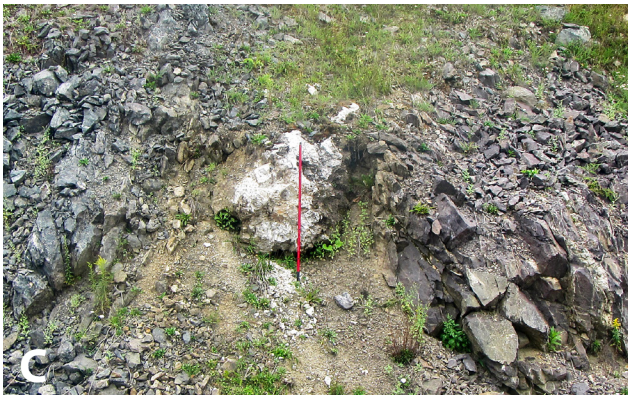

Figure 19. (A) The contact between the lapilli tuffs of stop 3 and the mafic flows of Cycle 2. The photograph was taken from the roadcut of basaltic lava flows on the east side of the Basin Road looking north toward the roadcut of basaltic lapilli tuff on the western side (Stop 3). The flows appear brown in the photo and are in conformable contact with the underlying basaltic lapilli tuff which is darker in colour. (B) Close up of an amygdaloidal portion of a flow (Loonie for scale). (C) The dark grey amygdaloidal basalt flows on the eastern side of the Basin Road are in fault contact to the south with maroon sedimentary rocks of Cycle 2. The fault zone contains a quartz vein about 70 cm wide. Veinlets of quartz cut the volcanic and sedimentary rocks near the faulted contact (Red measuring stick is about 1 m in length). Photos L. Fyffe.

Basin Access Road

Access via Hwy. 127 and Basin Road to Basin Access Road.

Stop1. Cycle 2 Volcaniclastic sedimentary rocks.
45° 11.5187′ N -66° 58.7239′ W

Volcaniclastic rocks of Cycle 2 are well exposed in an outcrop on the south side of the Basin Access Road, about 50 m west of the intersection with the Basin Road and also in another roadcut about 400 m farther west. This unit is up section from the Cycle 2 rocks exposed along the Basin Road and about 300 m to the south of faulted contact between the amygdaloidal basaltic flows and maroon sedimentary rocks of Cycle 2. The rocks are dark grey. Beds range in thickness from 10 to 50 cm and dip gently to the southwest (Fig. 20).

Stop 2. Cycle 2 Rhyolite pillow lobes
45° 11.6078′ N, 66° 58.9031′ W

This stop is about 400 m west of Stop 2. Here a pink, porphyritic, rhyolitic flow of Cycle 2 overlies the dark grey mafic volcaniclastic rocks observed at Stop 1. In contast, most of the other rhyolite flows in the area are crystal poor. The particularly interesting feature of this outcrop is the pillow-like structure of the rhyolite flow. These features could be flow lobes. Both subaerial and subaqueous rhyolite flows have marginal autobreccias. However, the nature of the margins, and association with marine sediments suggests that these are sub-aqueos rhyolite pilow flow lobes (Fig. 20).

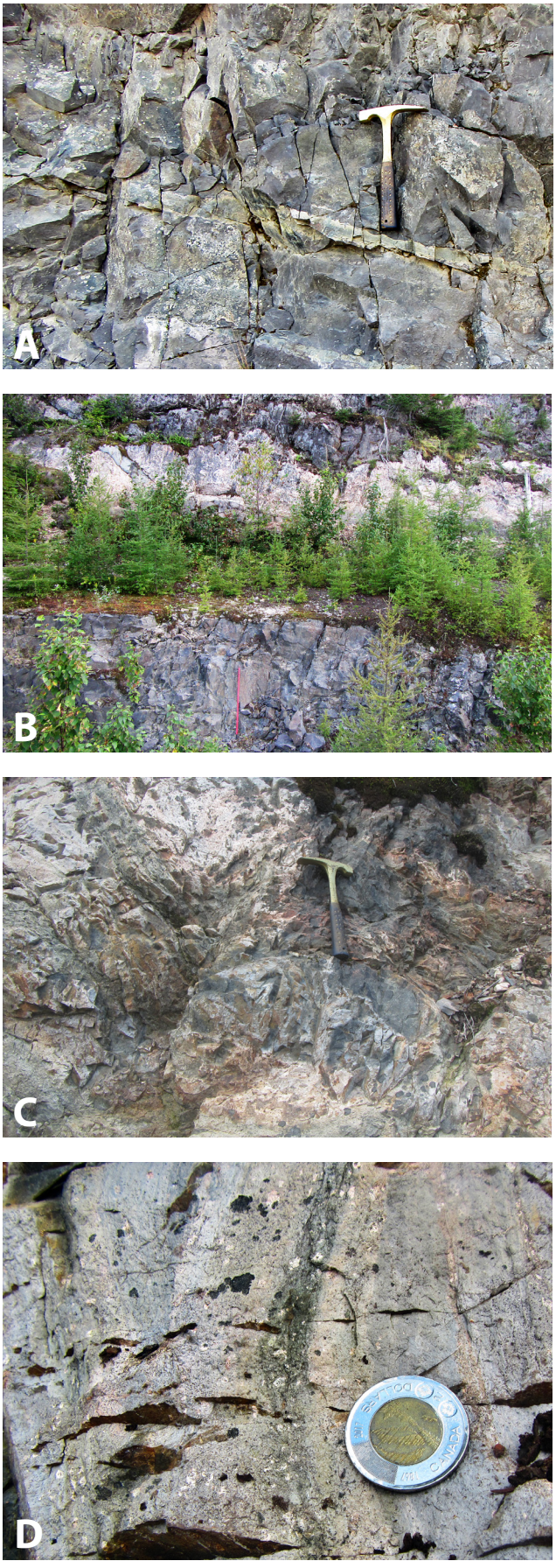

Figure 20. (A) Volcaniclastic rocks of stop 1. Load structures are present at the top of a 2 cm-thick olive green bed below the hammer handle. The presence of sparse, collapsed pumice shards suggests that this unit includes vitric tuffs. (B) A pink, porphyritic, rhyolitic flow of Cycle 2 in the centre of the photo overlies the dark grey mafic volcaniclastic rocks of Cycle 2 observed at Stop 1. A thick diabasic sill (upper centre of photograph) and thin, inclined diabasic dyke (upper left of photograph) cut the rhyolite (1 m measuring stick for scale). (C) These pillow-shaped lobes are about 1 m in length and 50 cm in height. Flow-layered rhyolite envelopes the lobes suggesting that they were entrained in the lava flow as it flowed. (D) Flow-banding in the porphyritic rhyolite showing it curving around the margin of the massive rhyolite lobes. Phenocrysts in the lava flow are alkali feldspar (Toonie for scale). Photos L. Fyffe.

Orrs Point/Paradox Point: Pulses of PDCs, Cycle 2

Access via Fiander Road from Hwy. 127. 45° 9.0148′ N, 66° 58.2739′ W to 45° 9.0207′ N, -66° 58.3534′ W

Rocks of the Devonian Perry Formation are exposed at the point. Follow these outcrops to the northwest. The Silurian section begins in the cove as indicted in the graphic log. Tides and time permiting we can continue past a fault that separates these pyroclastic units from a rhyolite flow (Figs. 21 and 22).

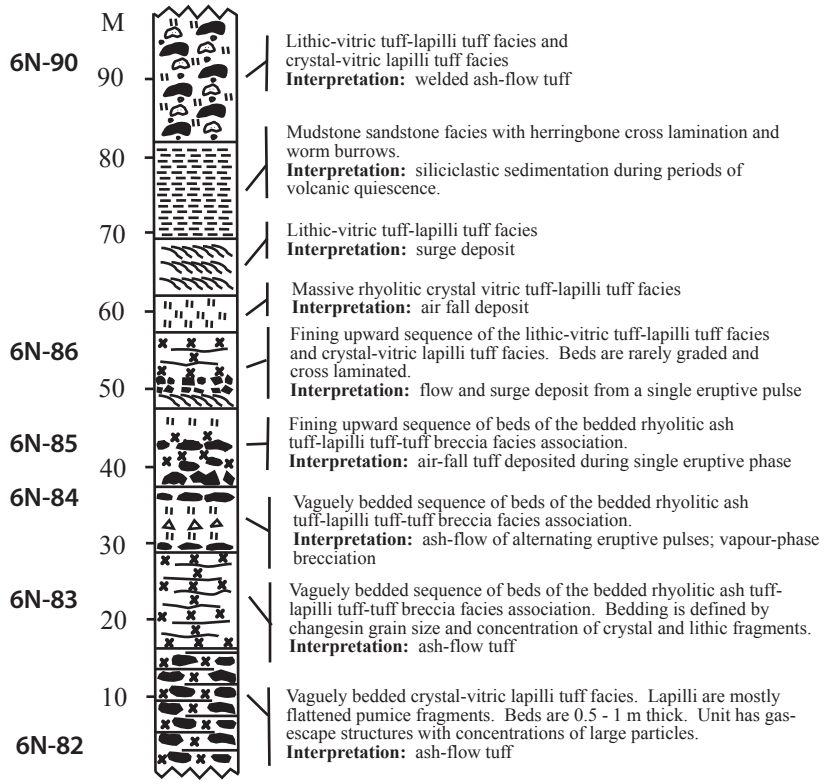

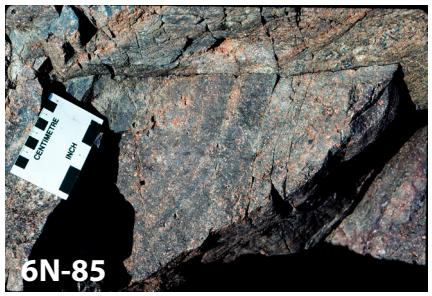

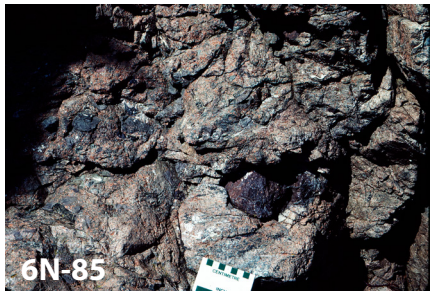

Figure 21. Graphical log through the Orrs Point tuffs from Van Wagoner, et a., (1994).

Photos S. Van Wagoner, et al.

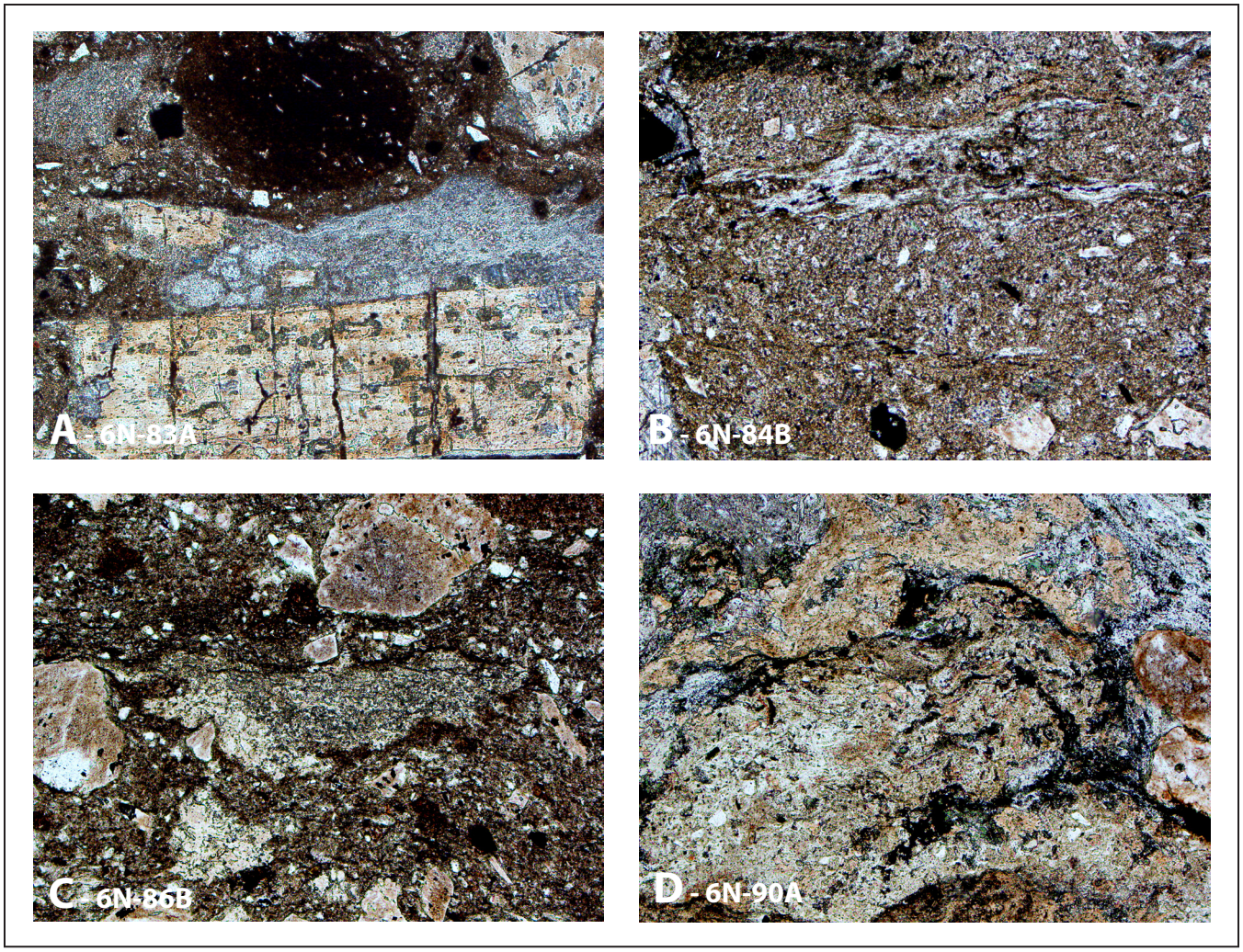

Figure 22. Four textures of pumice from Orrs point. Stratigaphic locations are shown on Fig. 21. (A) Pyrogenic crystal of plagioclase attached to pumice shard from heterolithic lapilli tuff, Bed 6N-83A. (B) Stretched pumice from Bed 6N-84B. (C) Heterolithic crystal tuff with flattened pumice but large crystals and lithics are not deformed, from Bed 6N-86B. (D) Strongly welded tuff with stretched and flattened pumice defining a flow foliation from 6N-90A. All photos at 5x, PPL, width of field is 2.2 mm. Photos N. Van Wagoner

Holts Point: Basaltic Styles of Volcanism, Cycle 3

Access via Holts Point Rd. from Hwy. 127. 45° 9.0414′ N, 66° 58.9918′ W to 45° 8.8867′ N, 66° 59.0315′ W
Optional: Highway 127 section which is along strike. 45° 10.3508′ N, 66° 59.5316′ W to 45° 10.6401′ N, 66° 59.3026′ W.

This field trip description is for Holts Point (Fig. 23).

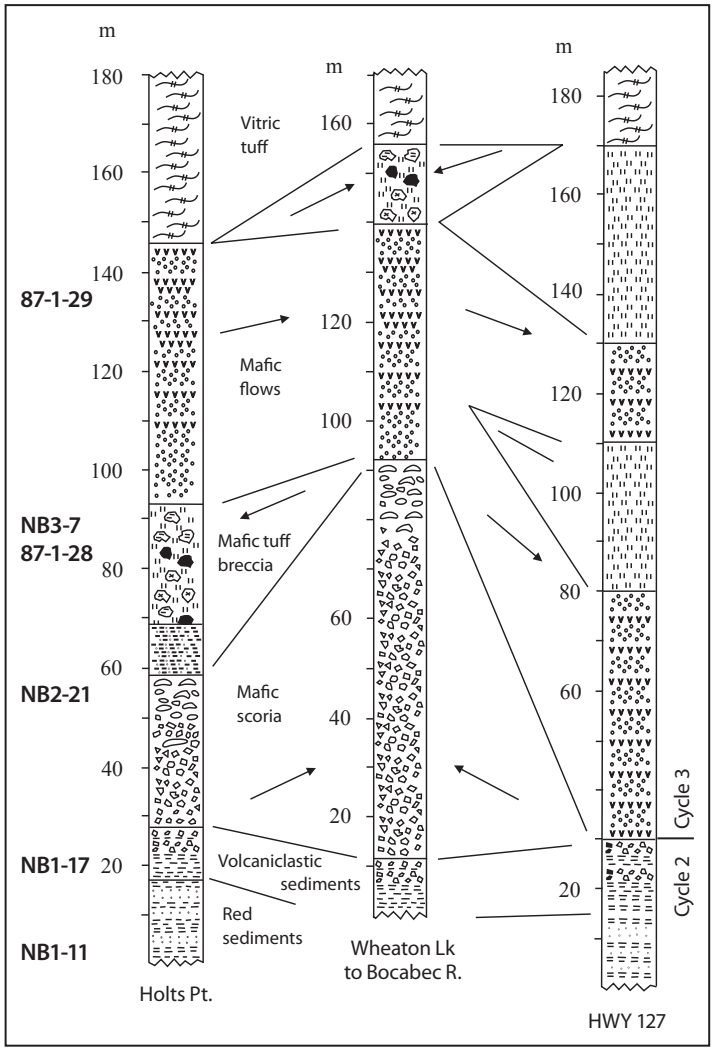

Figure 23. Schematic cross section of three sections through the mafic tuffs and flows of Cycle 3 and the underlying sediments. Holts point is the locality of this field trip stop. It is along strike with the section exposed along highway 127. The middle section extends from the eastern margin of Wheaton Lake, and west to Bocabec River (Modified from Van Wagoner et al., 1994).

If tides permit it is best to start at the most northern point, traversing up section as you walk to the southwest. This is a great traverse for looking at a sedimentary sequence, examples of Hawaiian and Strombolian styles of basaltic volcanism and the interaction of volcanics with sediments and shallow-level dikes (Fig. 23).

The lowermost unit is bedded red mudstone and siltstone, interbedded with volcaniclastic layers Holts Fig. 24 A). Bedding structures include shrinkage cracks, parallel, cross, and convolute lamination, current ripple marks and rain drop impressions (NB1-11). One bed is highly fossiliferous. The volcaniclastic beds include fragments of scoriaceous and massive basalt. These sediments were intruded by and interacted with vesicular dikes to form peperitic breccias at the dike margins.

Volcaniclastic layers increase up section until they comprise most of the sediment (Fig. 24 B) and that increases for the next ~7 m, followed by a deposit of basaltic scoria pyroclasts that contains accidental blocks of the underlying siltstone. The pyroclasts are ash to bomb-sized (up to 1 m in long dimension) and mostly scoriaceous. There is no matrix, but the unit is cemented by the agglutination of more fluid clasts and calcite. This unit was interpreted to be a scoria cone, characteristic of Strombolian-style volcanism (Van Wagoner et al., 1988)(Fig. 24 C).

This scoria is separated from the overlying tuff breccia by about 7 m of bedded red volcaniclastic siltstone. The next volcanic unit up section is a massive to vaguely bedded heterolithic basaltic tuff breccia. Clasts are up to 60% and up to 1 m in size, averaging 1-2 cm, and include siltstone, amygdaloidal and non-amygdaloidal basalt, gabbro, and rare cored bombs of lithic clasts rimmed by basalt (Fig. 24 D & E). The matrix is basaltic vitric tuff comprising angular bubble wall shards altered to chlorite. On the basis of shard morphology, the variety and abundance of accidental components and the size and shape of the fragments, this unit was interpreted to be an air-fall deposit from a phreatomagmatic eruption. (Van Wagoner et al., 1988).

Overlying these deposits from explosive eruptions, is a sequence about 50 m thick of basaltic pahoehoe flows, marking the end of mafic volcanism for this cycle (Fig. 24 F).

The overlying vitric tuff is not exposed at this location.

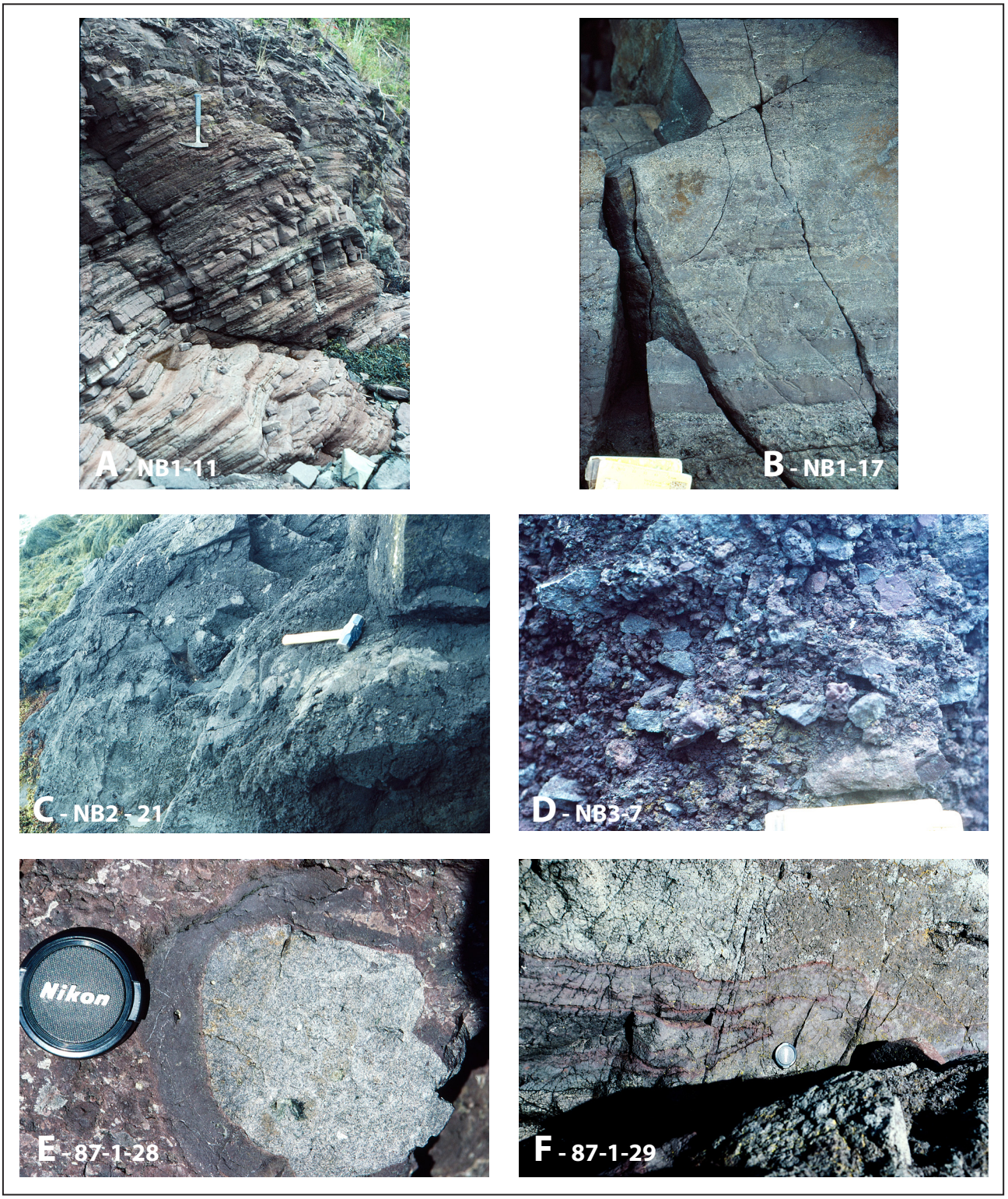

Figure 24. (A) General view of interbedded siltstone and mudstones of the sediment at the base of the basaltic volcanics of Cycle 3. (B) Bedded volcaniclastic siltstone. (C) Mafic scoria with large bomb. (D) Mafic tuff breccia showing the variety of clasts and their angularity. (E) Cored bomb in the mafic breccia. (F) Pahoehoe flow toes. Photos A-E N. Van Wagoner. Photo F W. McNeil.

Creighton Point: Cycles 3 and 4 Rhyolitic Effusive and Explosive Volcanism and Associated Sedimentary Rocks

Access from Hwy 127 via Holts Point Road to Mill Cove Branch Road (keep to the right). This traverse is on the Bocabec Cove side of Creighton Point. 45° 8.9340′ N, 67° 0.3600′ W

Stop 1. Sedimentary rocks on the beach just north of the old house at the end of the road: Interbedded red conglomerate, siltstone and mudstone. Primary structures include current ripple marks, oscillation ripples, rain drop impressions, and mud cracks. Clasts pebble-size and greater include vesicular basalt, porphyritic rhyolite, diabase, mudstone, siltstone and sandstone (Fig. 25).

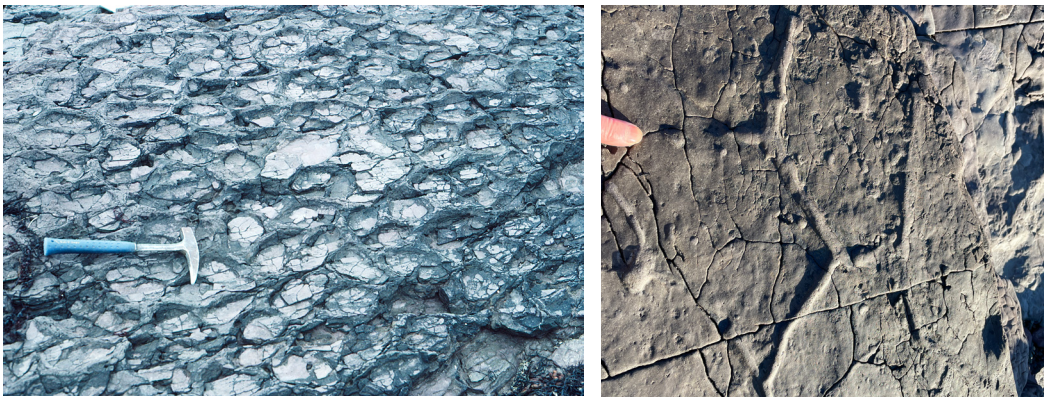

Figure 25. Mudcracks in the sedimentary rocks near the old house. Photo (left) N. Van Wagoner, (right) S. Van Wagoner.

Stop 2. Walk around the small cove to the north to view the brecciated contact between the sediments from the previous outcrop and a rhyolite flow.

At this locality is the margin of a rhyolite flow or dome of Cycle 4. The unit is about 400 m thick and tabular with peperitic breccia exposed at this locality and at Hansen Point to the north. This unit was interpreted as intrusive dome-like, based mainly on the peperitic and brecciated nature of the contacts. Features indicating that this is a peperitic breccia formed by interaction of lava with wet sediment, as opposed to sediment infilling an autobreccia, include shards of rhyolite in the clastic dikes. Perlitic cracks and spherulites in the rhyolite attest to its original glassy state. Ignimbrites typically do not produce basal breccias but rather have vitric and relatively planar lower contacts (Fig.26).

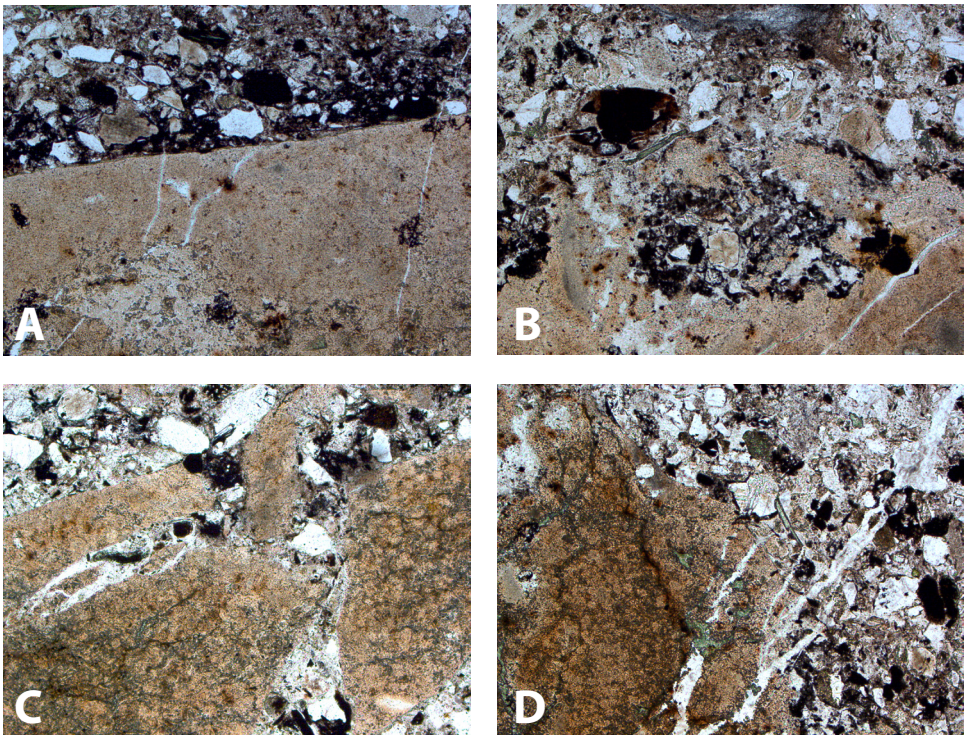

Figure 26. (A) Planar contact between rhyolite and sediment (note the pumice included in the rhyolite. (B) Interaction between the sediment and rhyolite with apophyses of rhyolite protruding into the sediment. (C) Fragments of rhyolite in the sediment. (D) Curviplanar margins of a rhyolite fragment in sediment. All images are at 5x, PPL, width of field is 2.2mm. Samples collected by M. Thicke. Photos N. Van Wagoner.

Stop 3. This is a down section traverse along the beach to the south through sediments, a portion of the rhyolite flow, and bedded tuffs.

As you walk around the point to the south look for lens-shaped beds of conglomerate.

The next contact is with a brecciated rhyolite, followed by less brecciated parts of the rhyolite flow. The rhyolite here is a relict glass with spherulites and, typical of this unit most of the felsic flows in the area, it is almost aphyric (Fig. 27).

Continuing to the south, the most distinctive unit along this section of the Bocabec Cove is a distinctly layered ash tuff, lapilli tuff and tuff breccia. Layers are 5 cm to 1 m thick and mostly non-welded to moderately welded. Some beds are internally laminated or graded and separated by fine ash beds that are altered to clay. Like the pyroclastic flows at Oven Head, these units also contain both basaltic and rhyolitic juvenile clasts (Fig. 28).

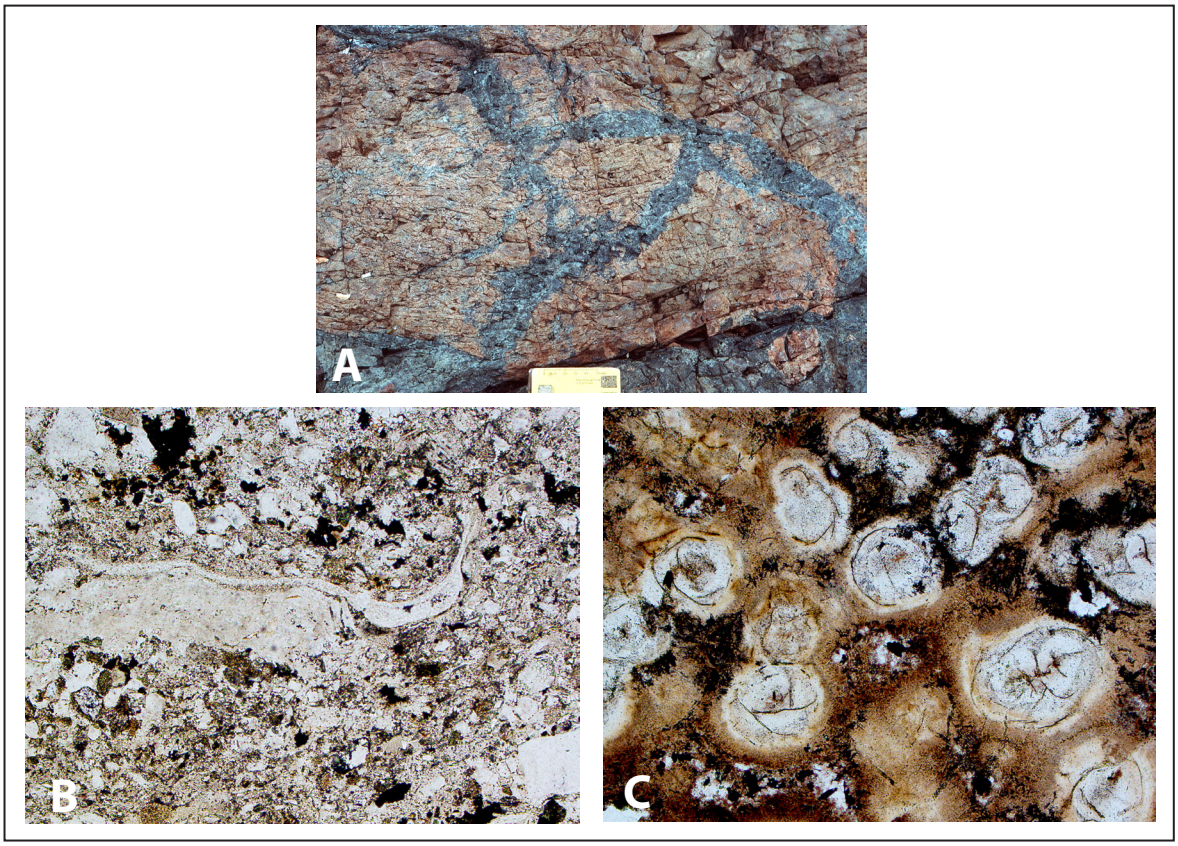

Figure 27. (A) In-situ breccia in a rhyolite flow. (B) Sediment from a brecciated contact with the rhyolite flow. This thin section photo shows a delicate rhyolite glass shard in sediment. (C) Photomicrograph of spherulitic rhyolite. Photos at 5x, PL, width of field is 2.2 mm. Photos N. Van Wagoner

Figure 28. (A) Bedded tuff and lapilli tuff. (B) Juvenile basaltic bomb in bedded rhyolitic vitric tuff. (C) Lapilli tuff to tuff breccia with large pumice. (D) Lapilli tuff and tuff breccia with juvenile pyroclasts of rhyolite and basalt. (E) Photomicrograph of a pumice fragment in the vitric matrix of a lapilli tuff. Photos at 5x, PL, width of field is 2.2 mm. Photos A-D S. Van Wagoner. Photo E N. Van Wagoner.

References

Baldwin, D. 1991. Physical volcanology, geochemistry, and depositional setting of the Siluro-Devonian volcanic rocks near St. Andrews, New Brunswick, MSc. Thesis, Acadia University, 231 p.

Bradley, D.C., Tucker, R.D., Lux, D., Harrris, A.G., and McGregor, D.C., 2000. Migration of the Acadian Orogen and foreland basin across the Northern Appalachians of Maine and adjacent areas. U.S. Geological Survey Professional Paper 1624, 49 p., https:// doi .org /10 .3133 /pp1624.

Branney et al. 2008 Branney, M.J., Bonnichsen, B., Andrews, G.D.M., Ellis, B., Barry, T.L. and McCurry, M. 2008. 'Snake River (SR)-type' volcanism at the Yellowstone hotspot track: Distinctive products from unusual, high-temperature silicic super-eruptions. Bulletin of Volcanology, 70, 293–314, https://doi.org/10.1007/s00445-007-0140-7.

Breitkreuz, C. 2013. Spherulites and lithophysae-200 years of investigation on high-temperature crystallization domains in silica-rich volcanic rocks. Bulletin of Volcanology, 75, 1–16, https://doi.org/10.1007/s00445-013-0705-6.

Brown. R.J., and Andrews, G.D,M. 2015. Deposits of pyroclastic density currents. in The Encyclopedia of Volcanoes, Sigurdsson, et. al. (eds). Chapt. 36, 631-648.

Brown, R.J., Branney, M.J., Maher, C. and Dávila-Harris, P. 2010. Origin of accretionary lapilli within ground-hugging density currents: Evidence from pyroclastic couplets on Tenerife. Bulletin of the Geological Society of America, 122, 305–320, https:// doi.org/10.1130/B26449.1.

Bryan, S.E., Peate, I.U., et al. 2010. The largest volcanic eruptions on Earth. Earth-Science Reviews, 102, 207–229, https://doi. org/10.1016/j.earscirev.2010.07.001.

Cas, R.A.F. and Wright, J.V., 1987. Volcanic successions: modern and ancient. Allen and Unwin, London, 528p.

Churchill-Dickson, L. 2004. A Late Silurian (Pridolian) age for the Eastport Formation, Maine: A review of the fossil, stratigraphic, and radiometric-age data. Atlantic Geology, 40, 189–195, https://doi.org/10.4138/1038.

Cimarelli, C., De Rita, D., Dolfi, D. and Procesi, M. 2008. Coeval strombolian and vulcanian-type explosive eruptions at Panarea (Aeolian Islands, Southern Italy). Journal of Volcanology and Geothermal Research, 177, 797–811, https://doi.org/10.1016/j. jvolgeores.2008.01.051.

Dadd, K.A. and Van Wagoner, N.A. 2002. Magma composition and viscosity as controls on peperite texture: An example from Passamaquoddy Bay, southeastern Canada. Journal of Volcanology and Geothermal Research, 114, 63-80, https://doi. org/10.1016/S0377-0273(01)00288-8.

Dostal, J., Wilson, R.A. and Keppie, J.D. 1989. Geochemistry of Siluro-Devonian Tobique volcanic belt in northern and central New Brunswick (Canada): tectonic implications. Canadian Journal of Earth Sciences, 26, 1282–1296, https://doi.org/10.1139/e89-108.

Dufek, J., Ongaro, T. E., and Roche, O. 2015. Pyroclastic density currents: processes and models. in The Encyclopedia of Volcanoes. (Academic Press), 617–629.

Dunn, T and Stringer P., 1990. Petrology and petrogenesis of the Ministers Island dike, southwest New Brunswick. Contributions to Mineralogy and Petrology, 105, 55-65.

Fyffe, L.R., and Fricker, A. 1987. Tectonostratigraphic terrane analysis of New Brunswick. Atlantic Geology, 23, pp. 113–122.

Fyffe, L.R., Pickerill, R.K. and Stringer, P. 1999. Stratigraphy, sedimentology and structure of the Oak Bay and Waweig Formations, Mascarene Basin: Implications for the paleotectonic evolution of southwestern New Brunswick. Atlantic Geology, 35, 59–84, https://doi.org/10.4138/2024.

Gençalio lu-Kuşcu, G., Atilla, C., Cas, R.A.F. and Kuşcu, I. 2007. Base surge deposits, eruption history, and depositional processes of a wet phreatomagmatic volcano in Central Anatolia (Cora Maar). Journal of Volcanology and Geothermal Research, 159, 198–209, https://doi.org/10.1016/j.jvolgeores.2006.06.013.

Gilbert, J.S. and Lane, S.J. 1994. The origin of accretionary lapilli. Bulletin of Volcanology, 56, 398–411, https://doi.org/10.1007/ BF00326465.

Greeley. R., 1982. The Snake River Plain, Idaho: representative of a new category of volcanism. Journal of Geophysical Research 87(B4):2705–2712

Henry, C.D. and Wolff, J.A. 1992. Distinguishing strongly rheomorphic tuffs from extensive silicic lavas. Bulletin of Volcanology, 54, 171–186, https://doi.org/10.1007/BF00278387..

Le Bas, M.J., Le Maitre, R.N., Streckeisen, A. and Zanettin, B. 1986. A chemical classification of volcanic rock based on total silica diagram. Journal Petrology, 27, 745–750.

McLaughlin, K.J., Barr, S.M., Hill, M.D., Thompson, M.D., Ramezani, J. and Reynolds, P.H. 2003. The Moosehorn Plutonic Suite, southeastern Maine and southwestern New Brunswick: Age, petrochemistry, and tectonic setting. Atlantic Geology, 39, 123–146, https://doi.org/10.4138/1176.

McNeil, W. 1989. The physical volcanology and geochemistry of the eastern portion of the volcanic belt of Passamaquoddy Bay, southwestern New Brunswick, MSc Thesis, Acadia University, 197 p.

Mohammadi, N., Fyffe, L., McFarlane, R.M., Thorne, K., Lentz, D., Charnley, B., and Branscombe, L., and Butler, S. 2017. Geological relationships and laser ablation ICP-MS U-Pb geochronology of the Saint George Batholith , southwestern New Brunswick , Canada : implications for its tectonomagmatic evolution. Atlantic Geology, 53, 207–240, https://doi.org/10.4138/atlgeol.2017.00.

Mohammadi, N., Fyffe, L., McFarlane, C., Wilson, R. and Lentz, D., 2019. U-Pb zircon and monazite geochronology of volcanic and plutonic rocks in southwestern, central, and northeastern New Brunswick. Geological Survey of Canada Open File 8581, 44 p.

Moore, J.G., and Peck, D.L., 1962. Accretionary lapilli in volcanic rocks of the western continental United States. The Journal of Geology, 70, 182–194.

Moore, J.G., Nakamura, K., and Alcarez, A. 1966. The 1965 eruption of Taal Volcano: Science, 151, 955–960. doi: 10.1126/science.151.3713.955.

Mueller, S.B., Kueppers, U., Ayris, P.M., Jacob, M. and Dingwell, D.B. 2016. Experimental volcanic ash aggregation: Internal structuring of accretionary lapilli and the role of liquid bonding. Earth and Planetary Science Letters, 433, 232–240, https://doi.org/10.1016/j.epsl.2015.11.007.

Naik, A., Sheth, H., Sheikh, J.M. and Kumar, A. 2021. Extremely high-grade, lava-like rhyolitic ignimbrites at Osham Hill, Saurashtra, northwestern Deccan Traps: Stratigraphy, structures, textures, and physical volcanology. Journal of Volcanology and Geothermal Research, 419, 107389, https://doi.org/10.1016/j.jvolgeores.2021.107389.

Pearce, J.A. and Norry, M.J. 1979. Petrogenetic implications of Ti, Zr, Y, and Nb variations in volcanic rocks. Contributions to Mineralogy and Petrology, 69, 33–47, https://doi.org/10.1007/BF00375192.

Pearce, J.A., Harris, N.B.W. and Tindle, A.G. 1984. Trace element discrimination diagrams for the tectonic interpretation of granitic rocks. Journal of Petrology, 25, 956–983, https://doi.org/10.1093/petrology/25.4.956.

Pickerill, R.K. and Pajari, G.E., 1976. The Eastport Formation (Lower Devonian) in the northern Passamaquoddy Bay area, southwest New Brunswick. Canadian Journal of Earth Science, 13, 266-270.

Piñan-Llamas, A.P. and Hepburn, J.C. 2013. Geochemistry of Silurian-Devonian volcanic rocks in the Coastal Volcanic belt, Machias-Eastport area, Maine: Evidence for a pre-Acadian arc. Bulletin of the Geological Society of America, 125, 1930–1942, https://doi.org/10.1130/B30776.1

Rankin, D.W., and Tucker, R., 1995. U-Pb age of the Katahdin -Traveler igneous suite, Maine, local age of the Acadian orogeny, and thickness of Taconian crust. Geological Society of America Abstracts with Programs, 27/6, 224–225.

Rosa, C.J.P., McPhie, J. and Relvas, J.M.R.S. 2016. Distinguishing peperite from other sediment-matrix igneous breccias : Lessons from the Iberian Pyrite Belt. Journal of Volcanology and Geothermal Research, 315, 28–39, https://doi.org/10.1016/j.jvolgeores.2016.02.007.

Sánchez-Mora, D., McFarlane, C.R.M., Walker, J.A. and Lentz, D.R. 2021. Geochemistry and U-Pb geochronology of the Williams Brook area, Tobique–Chaleur zone, New Brunswick: Stratigraphic and geotectonic setting of gold mineralization. Canadian Journal of Earth Sciences, 58, 1040–1058, https://doi.org/10.1139/cjes-2020-0094.

Schmid, R., 1981. Descriptive classification and nomenclature of pyroclastic deposits and fragments: Recommendations of the IUGS Subcommission on the Systematics of Igneous Rocks. Geology, 9, 41-43.

Scarpati, C., Sparice, D. and Perrotta, A. 2020. Dynamics of large pyroclastic currents inferred by the internal architecture of the Campanian Ignimbrite. Scientific Reports, 10, 1–13, https://doi.org/10.1038/s41598-020-79164-7.

Schumacher, R. and Schmincke, H.U. 1991. Internal structure and occurrence of accretionary lapilli - a case study at Laacher See Volcano. Bulletin of Volcanology, 53, 612–634, https://doi.org/10.1007/BF00493689.

Seaman, S.J., Wobus, R.A., Wiebe, R.A., Lubick, N., and Bowring, S.A., 1995, Volcanic expression of bimodal magmatism: The Cranberry Island Series–Cadillac Mountain Complex, coastal Maine: The Journal of Geology, v. 103, p. 301–311, https:// doi .org /10 .1086 /629748.

Seaman, S.J., Scherer, E.E., Wobus, R.A., Zimmer, J.H., and Sales, J.G., 1999, Late Silurian volcanism in coastal Maine: The Cranberry Island series: Geological Society of America Bulletin, v. 111, p. 686–708, https:// doi .org /10 .1130 /0016 -7606 (1999)111 <0686: LSVICM>2 .3 .CO;2.

Seaman, S.J., Hon, R., et al. 2019. Late paleozoic supervolcano-scale eruptions in Maine, USA. Bulletin of the Geological Society of America, 131, 1995–2010, https://doi.org/10.1130/B32058.1.

Seebeck, H., Nicol, A., Villamor, P., Ristau, J. and Pettinga, J. 2014. Structure and kinematics of the Taupo Rift, New Zealand. Tectonics, 33, 1178–1199, https://doi.org/10.1002/2014TC003569.

Sheikh, J.M., Sheth, H., Naik, A. and Keluskar, T. 2020. Widespread rheomorphic and lava-like silicic ignimbrites overlying flood basalts in the northwestern and northern Deccan Traps. Bulletin of Volcanology, 82, https://doi.org/10.1007/s00445-020-01381-9.

Textor, C., Graf, H.F., Herzog, M., Oberhuber, J.M., Rose, W.I. and Ernst, G.G.J. 2006a. Volcanic particle aggregation in explosive eruption columns. Part I: Parameterization of the microphysics of hydrometeors and ash. Journal of Volcanology and Geothermal Research, 150, 359–377, https://doi.org/10.1016/j.jvolgeores.2005.09.007.

Textor, C., Graf, H.F., Herzog, M., Oberhuber, J.M., Rose, W.I. and Ernst, G.G.J. 2006b. Volcanic particle aggregation in explosive eruption columns. Part II: Numerical experiments. Journal of Volcanology and Geothermal Research, 150, 378–394, https://doi.org/10.1016/j.jvolgeores.2005.09.008.

Tomita, K., Kanai, T., Kobayashi, T. and Oba, N. 1985. Accretionary lapilli formed by the eruption of Sakurajima volcano. Journal of the Japanese Association of Mineralogists, Petrologists and Economic Geologists, 80, 49–54, https://doi.org/10.2465/ganko1941.80.49.

Turner, S. and Burrow, C.J. 2018. Microvertebrates from the Silurian – Devonian boundary beds of the Eastport Formation, Maine, eastern USA. Atlantic Geology, 54, 171–187, https://doi.org/10.4138/atlgeol.2018.006.

van Staal, C.R. and Barr, S.M. 2012. Lithospheric architecture and tectonic evolution of the Canadian Appalachians and associated Atlantic margin. In Tectonic Styles in Canada: the LITHOPROBE perspective, Geological Association of Canada Special Paper, 49, 41–95.

van Staal, C.R., Whalen, J.B., Valverde-Vaquero, P., Zagorevski, A., and Rogers, N. 2009. Pre-Carboniferous, episodic accretion-related, orogenesis along the Laurentian margin of the northern Appalachians. Geological Society, London, Special Publications, 327, 271-316. https://doi.org/10.1144/SP327.13.

van Staal, C.R., Zagorevski, A., McNicoll, V.J. and Rogers, N. 2014. Time-transgressive Salinic and Acadian orogenesis, magmatism and Old Red Sandstone sedimentation in Newfoundland. Geoscience Canada, 41, 138–164, https://doi.org/10.12789/geocanj.2014.41.031.

Van Wagoner, N. A., and Dadd, K.A. 2003. A Silurian age for the Passamaquoddy Bay volcanic sequence in southwestern New Brunswick: implications for regional correlations. Geological Society of America Abstracts with Programs. 35:3, 79.

Van Wagoner, N.A., McNeil, W., Fay, V.K., 1988. Early Devonian bimodal volcanic rocks of southwestern New Bruns- wick: petrography, stratigraphy, and depositional setting. Martime Sediments and Atlantic Geology, 24, 301-319.

Van Wagoner, N. A., Dadd, K. A., Baldwin, D. K., McNeil, W. 1994. Physical volcanology, stratigraphy, and depositional setting of the middle Paleozoic volcanic and sedimentary rocks of Passamaquoddy Bay, southwestern New Brunswick. Geological Survey of Canada Paper, 91–14, 53.

Van Wagoner, N.A., Leybourne, M.I., Dadd, K.A. and Huskins, M.L.A. 2001. The Silurian(?) Passamaquoddy Bay mafic dyke swarm, New Brunswick: Petrogenesis and tectonic implications. Canadian Journal of Earth Sciences, 38, 1565–1578, https://doi.org/10.1139/cjes-38-11-1565.

Van Wagoner, N.A., Leybourne, M.I., Dadd, K.A., Baldwin, D.K. and McNeil, W. 2002. Late Silurian bimodal volcanism of southwestern New Brunswick Canada: Products of continental extension. Bulletin of the Geological Society of America, 114, https://doi.org/10.1130/0016-7606(2002)114<0400:LSBVOS>2.0.CO;2.

Van Wagoner, N. A., and Dadd, K. A., in prep, Snake River-type volcanism in a Peri-tidal environment: Late Silurian Eastport Formation, Passamaquoddy Bay bimodal volcanic sequence, New Brunswick, Canada.

White, J.D.L. and Valentine, G.A. 2016. Magmatic versus phreatomagmatic fragmentation: Absence of evidence is not evidence of absence. Geosphere, 12, 1478–1488, https://doi.org/10.1130/GES01337.1.

White, J.D.L., Bryan, S.E., Ross, P.S., Self, S. and Thordarson, T. 2009. Physical volcanology of continental large igneous provinces: Update and review. Special Publications of IAVCEI, 291–321, https://doi.org/10.1144/iavcel002.15.

Wilson, R.A., van Staal, C.R., and Kamo, S.L. 2017. Rapid transition from the Salinic to Acadian orogenic cycles in the northern Appalachian Orogen: Evidence from northern New Brunswick, Canada. American Journal of Science, 317 (4) 449-482. DOI: https://doi.org/10.2475/04.2017.02

Winchester, J.A., and Floyd, P.A. 1977. Geochemical discrimination of different magma series and their differentiation products using immobile elements. Chemical Geology, 20, 325–343.

Acknowledgements

NVW wishes to thank Mike Thicke for his extraordinary mapping and field support during the summer of 1987. Mike made an outstanding contribution to the project and the morale of the team.

She also thanks her former students who worked in the area: honours students, David Lowe, Robert Lodge, Miranda Huskins, and Terry Lawrence; MSc. students and co-authors, Wayne McNeil and Diane Baldwin; and Kelsie Dadd (former Postdoctoral Associate and co-author); and field assistants, Matthew Leybourne and Mario Justino. It was a great privilege and pleasure to work with such a talented group of people at Acadia University.

Madeline Rein (Thompson Rivers University) is thanked for lab assistance in the preparation of this guide.

LF thanks his field assistant, Jolane Sorge.

Steve Van Wagoner is thanked for the layout and graphic design of the manuscript, and decades of dedicated field assistance.

The initial work was funded by NSERC operating grants and a Canada-New Brunswick Mineral Development Agreement grant to NVW.

This field guide is dedicated to the memory of Mike Thicke

Graduate of Acadia University (MSc 1987)